Energies **2015**, *8*, 859-894; doi:10.3390/en8020859

OPEN ACCESS

energies

ISSN 1996-1073

www.mdpi.com/journal/energies

Review

Supercritical Water Gasification of Biomass: A Literature and Technology Overview

Onursal Yakaboylu [1,*], John Harinck [1,2], K. G. Smit [2] and Wiebren de Jong [1]

[1] Faculty of Mechanical, Maritime and Materials Engineering, Process and Energy Department, Delft University of Technology, Leeghwaterstraat 39, NL-2628 CA Delft, The Netherlands; E-Mails: j.harinck@gensos.nl (J.H.); wiebren.dejong@tudelft.nl (W.J.)

[2] Gensos B.V., Wijdenes Spaansweg 57, NL-1764 GK Breezand, The Netherlands; E-Mail: k.g.smit@gensos.nl

***** Author to whom correspondence should be addressed; E-Mail: o.yakaboylu@tudelft.nl; Tel.: +31-15-27-82186.

Academic Editor: Thomas E. Amidon

Received: 26 November 2014 / Accepted: 16 January 2015 / Published: 27 January 2015

Abstract: The supercritical water gasification process is an alternative to both conventional gasification as well as anaerobic digestion as it does not require drying and the process takes place at much shorter residence times; a few minutes at most. The drastic changes in the thermo-physical properties of water from the liquid state to the supercritical state make it a promising technology for the efficient conversion of wet biomass into a product gas that after upgrading can be used as substitute natural gas. The earliest research goes back as far as the 1970s and since then, supercritical water has been the subject of many research works in the field of thermochemical conversion of wet biomass. This article reviews the state of the art of the supercritical water gasification technology starting from the thermophysical properties of water and the chemistry of reactions to the process challenges of such a biomass based supercritical water gasification process plant.

Keywords: biomass; supercritical water; gasification; hydrothermal

---

1. Introduction

Ever since the industrial revolution, global energy demand and consumption has increased drastically and it is predicted to increase even more in the near future. U.S. Energy Information Administration [1] foresees a 56% increase in the world energy consumption as well as in the natural gas demand in the following 30 years. In OECD Europe, natural gas consumption will increase from 540 to 680 billion cubic meters from 2015 to 2040. In contrast, the natural gas production in OECD Europe will increase only from 254 to 280 billion cubic meters. It is a fact that with such consumption rates, the fossil fuel reserves will eventually deplete.

It is not only the depletion problem that the fossil fuels face. More importantly, fossil fuels are associated with environmental problems. CO_2 emissions already increased from 21.5 to 33.5 billion metric tons from 1990 to 2014, and in 2040 it is expected to reach 45.5 billion metric tons of which 10 billion metric tons originate come from natural gas [1].

Fortunately, the interest in renewable energy is also increasing. Consumption of renewable energy will double and the share of the renewables in the world's energy consumption is expected to increase from 11% in 2010 to 15% in 2040 [1].

Biomass will play an important role among the other renewable energy sources globally as it is already the fourth largest energy resource after coal, oil and natural gas [2]. Furthermore, in particular, non-food ligno-cellulosics are among the most sustainable energy sources which have the potential to decrease fossil fuel consumption. It is possible to obtain gaseous, liquid or solid biofuels from biomass via thermochemical or biochemical conversion routes [3]. Thermochemical conversion consists of pyrolysis, liquefaction, gasification and combustion, whereas biochemical conversion consists of fermentation and digestion [4]. Among them, gasification is one of the most favorable options as the products can serve all types of energy markets: heat, electricity and transportation [3].

However, in case of wet biomass with a high moisture content, it results in a negative impact on the energy efficiency of the gasification process due to the fact that drying costs more energy than the energy content of the product for some biomass types. An alternative method applied for the conversion of wet biomass such as sewage sludge, cattle manure and food industry waste is anaerobic digestion. This process is however characterized by a slow reaction and typical residence times are almost 2–4 weeks. Besides, the fermentation sludge and wastewater from the reactors should further be treated.

The supercritical water gasification process is an alternative to both conventional gasification as well as the anaerobic digestion processes for conversion of wet biomass. This process does not require drying and the process takes place at much shorter residence times; a few minutes at most [3,5]. Supercritical water gasification is therefore considered to be a promising technology for the efficient conversion of wet biomass into a product gas that after upgrading can be used as substitute natural gas. The earliest research goes back as far as the 1970s [6] and since then, supercritical water has been the subject of many research works regarding the thermochemical conversion of wet biomass [7–9]. This article reviews the state of the art in supercritical water gasification technology, starting from the thermophysical properties of water and the chemistry of reactions to the process challenges of such a supercritical water gasification of a biomass processing unit.

2. Properties of Near-Critical and Supercritical Water

The main reason for the interest in research on supercritical water concerns the favorable physical properties of water and the way they change in the supercritical region which causes water to act as a solvent as well as a catalyst. Furthermore, through hydrolysis reactions, water also acts as a reactant [10].

The critical point for pure water is 374 ℃ and 22.1 MPa [11]. Above this temperature and pressure, water is in its supercritical phase as shown in Figure 1.

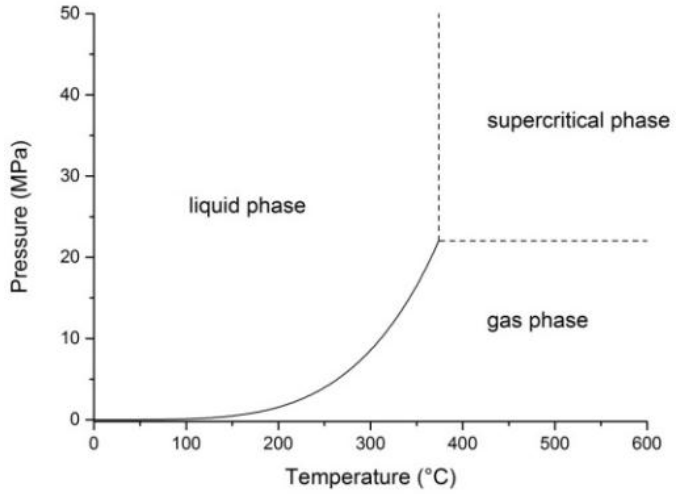

Figure 1. Schematic phase diagram of water; reprinted with permission from [12], copyright 2013 Elsevier.

Gasification of biomass is mainly influenced by the density, viscosity and dielectric constant of water. Above the critical point, physical properties of water drastically change and water behaves as a homogeneous fluid phase. In its supercritical state, water has a gas-like viscosity and liquid-like density, two properties which enhance mass transfer and solvation properties, respectively [3,13]. Figure 2 shows the dielectric constant and Figure 3 shows the density of water at various pressures and temperatures.

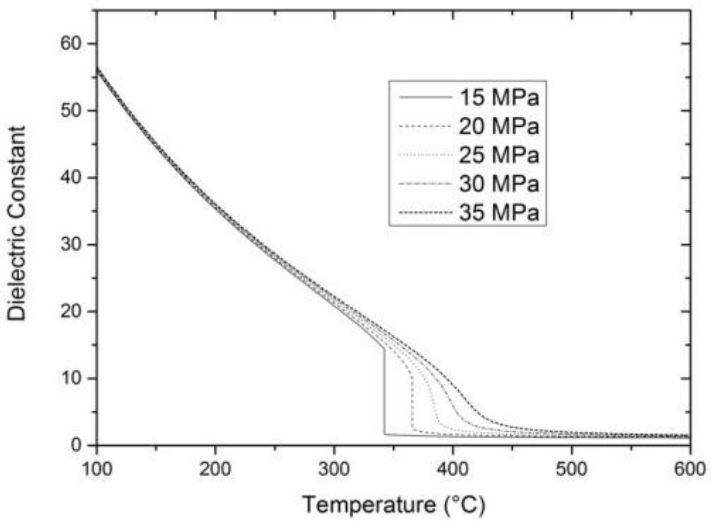

Figure 2. Dielectric constant of water at various temperatures and pressures; reprinted with permission from [12], copyright 2013 Elsevier.

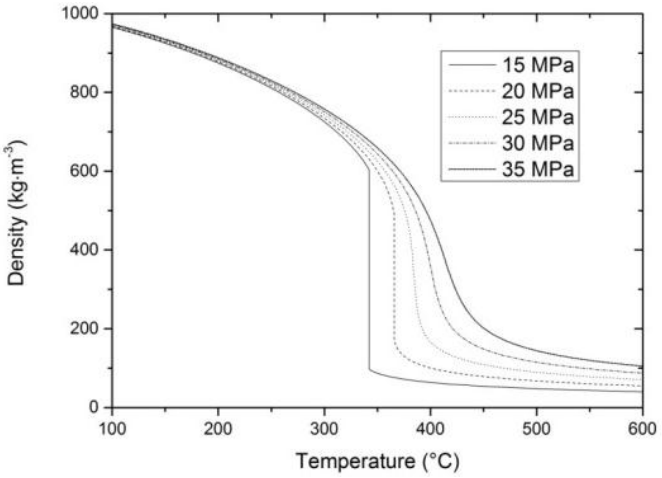

Figure 3. Density of water at various temperatures and pressures; reprinted with permission from [12], copyright 2013 Elsevier.

Liquid water at standard conditions (25 ℃ and 0.1 MPa) is an excellent polar solvent due to its high dielectric constant. It has a high solubility for many compounds and electrolytes; however, it is poorly miscible with hydrocarbons and gases. When water enters its supercritical phase, the dielectric constant drastically decreases. Water thus starts to behave like an organic, non-polar solvent which results in poor solubility for inorganics, and complete miscibility with gases and many hydrocarbons. Due to its miscibility, phase boundaries do not exist anymore. This absence leads to fast and complete homogeneous reactions of water with organic compounds [10,14]. Figure 4 shows the solubility of some salts and Figure 5 shows the solubility of benzene in supercritical water.

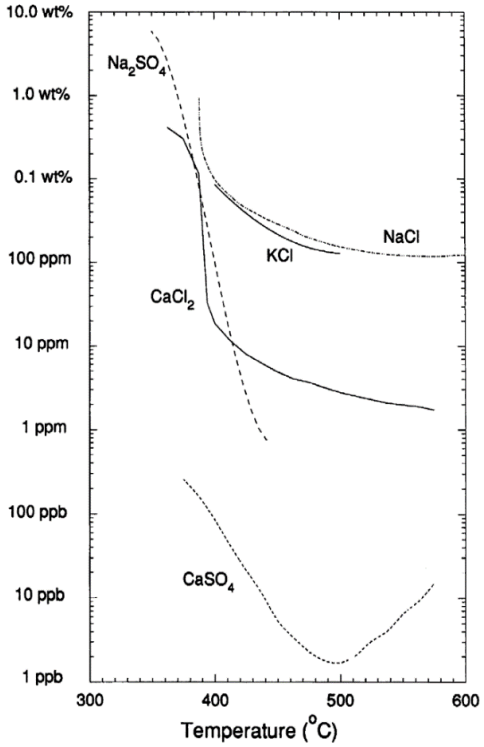

Figure 4. The solubility of limits of various salts at 25 MPa. Reprinted with permission from [9], copyright 2008 Royal Society of Chemistry, original data is from [15].

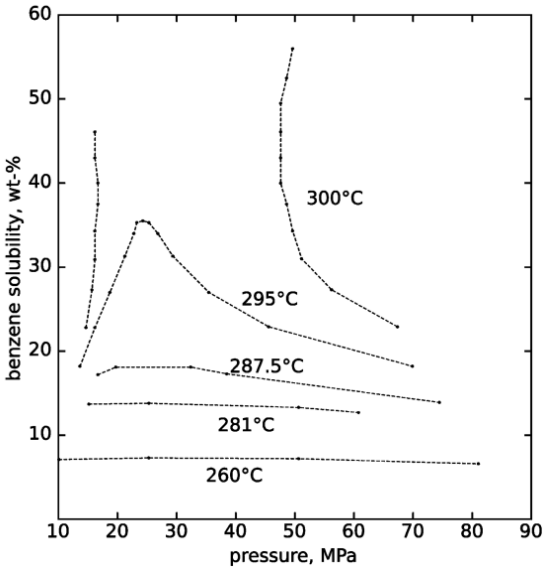

Figure 5. Benzene solubility in high-pressure water. Reprinted with permission from [9], copyright 2008 Royal Society of Chemistry, original data is from [16]. Please note that at 300 ℃ and above, the phases become completely miscible between 17 and 47 MPa.

Figure 6 shows the ionic product of water at different conditions. The ionic product of water increases with an increase in the pressure, however, the temperature shows a more complicated effect. At 25 MPa, the ionic product of water increases with temperature and reaches its highest value of 10^{-11} at a temperature of around 250 ℃. Starting from 250 ℃, it decreases slightly till the critical temperature, then reaches a value of 10^{-13} and it subsequently decreases drastically with the increase in temperature reaching a value of 10^{-23} at 600 ℃ [17]. When the ionic product of water is relatively high, water acts as an acid or base catalyst due to the high concentration of H_3O^+ and OH^- ions. At these conditions (liquid water, high pressure supercritical water and probably the dense gas phase), the main reaction pathways are ionic. However, when the ionic product of water is low (steam and less dense supercritical water), the main reactions are radical. Around the critical point of water, both ionic and radical reactions take place and compete with each other. It is concluded that when the ionic product is higher than 10^{-14}, aqueous phase ionic reactions preferably take place and when the ionic product is much lower than 10^{-14}, free radical gas phase reactions become dominant. Below the critical temperature, the rate of ionic reactions generally increases with an increase in temperature until the critical temperature is reached. Near the critical point, the reaction rate decreases drastically and shows a strong and characteristic non-Arrhenius behavior. At the critical point, the reaction rates can decrease or increase drastically depending on the chemistry [10,14,18].

Another interesting phenomenon that is observed concerning the thermophysical property of supercritical water is its change of the isobaric heat capacity, denoted with C_p. Figure 7 shows the isobaric heat capacity of water at various temperatures and pressures. Please note that at the critical point, C_p of water tends to approach infinity and becomes not measurable (the highest value of C_p given by [19] is at 373.91 ℃ with a value of 2.4355×10^5 J mol^{-1} K^{-1}). When the water shifts to its supercritical phase from liquid phase, its latent heat tends to zero. Instead, there is a high C_p value which mimics the high energy demand for the phase change. However, the increase in the pressure results in a decrease of the C_p value.

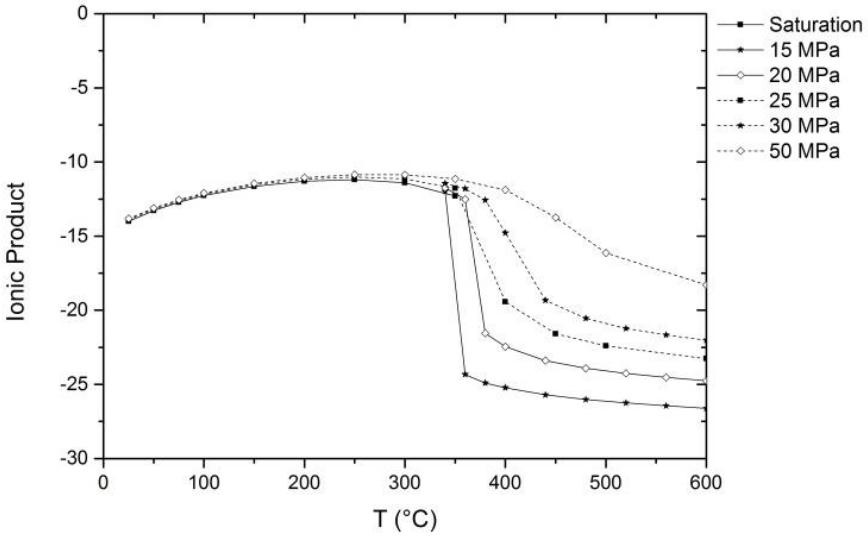

Figure 6. Ionic product of water at various temperatures and pressures; data taken from [17].

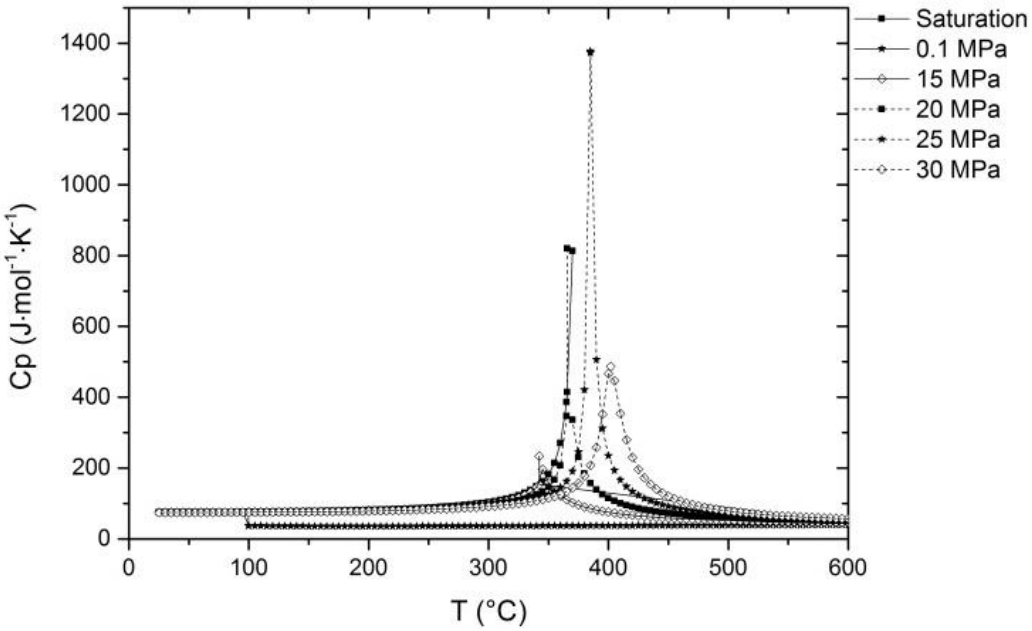

Figure 7. Isobaric heat capacity of water at various temperatures and pressures; data taken from [19].

The changes in the thermophysical properties of water, especially the disappearance of the phase boundaries and non-polar like solvent behavior, gives the opportunity for salt separation and tar-free gasification of biomass due to the salt precipitation, and dissolution and conversion of tar-precursors in a hydrothermal medium. The term hydrothermal refers to an aqueous system at temperatures and pressures near or above the critical point of water [13].

3. Hydrothermal Conversion of Organic Feedstocks

Hydrothermal conversion of biomass can be classified as carbonization, oxidation, liquefaction and gasification depending on the process parameters. Each of these routes results in different products varying from biochar to hydrogen rich gas [20–24]. Hereafter, they are briefly summarized.

3.1. Carbonization

Hydrothermal carbonization (HTC) is the (pre)treatment of lignocellulosic biomass in hot (180–280 °C) compressed water at residence times varying from minutes to hours. The solid product is hydrophobic and reported to be similar to lignite by means of ultimate analysis. Besides, it can be easily pelletized. By-products include aqueous sugars, acids, carbon dioxide and water [21].

3.2. Oxidation

Supercritical water oxidation (SCWO) has been the main research topic in the 1990s regarding the hydrothermal conversion of biomass. It is an effective technology for the treatment of organic compounds resulting in CO_2 and H_2O as the main products as well as N_2 when nitrogen containing compounds are treated. The process takes place at very short residence times (less than 50 s at around 650 °C). The main application of SCWO is the destruction of wastewaters and sludges [25,26].

3.3. Liquefaction

Hydrothermal liquefaction (HTL) is a technology which enables the conversion of biomass into clean liquid fuels (so called "biocrude" or "biooil"). The process takes place with the presence of water or water-containing solvent/co-solvent. The most efficient conversion can be obtained in the presence of a catalyst (mostly alkaline based) at a temperature of 200–400 °C and at a pressure 5–25 MPa. The process's oily product can be defined as a viscous crude oil replacement. However, it has been reported to show important differences as compared to conventional crude such as having a significantly higher oxygen content which (may) require an upgrading process [9,24].

3.4. Gasification

Gasification of organic feedstocks in a hydrothermal medium can be performed at different temperatures and pressures, or in the presence of a catalyst. It can be a catalytic gasification process at subcritical conditions (225–265 °C and 2.9–5.6 MPa) [27], a low temperature catalytic gasification process at supercritical conditions (near critical temperatures to ~500 °C) and a high temperature non-catalytic gasification process (at temperatures higher than 500 °C) [9]. It has significant advantages over the other biomass conversion routes by means of heat utilization when the moisture content of the feedstocks exceeds 30 wt%. Figure 8 shows the comparison of supercritical water gasification (SCWG) with the other biomass conversion routes on heat utilization efficiency basis. Another comparison between conventional gasification and SCWG can be made based on the works of Gassner *et al.* [28] and van der Meijden *et al.* [29]. Here, both of the authors investigated the energy efficiencies of wood gasification processes. The results of Gassner *et al.* [28] showed that the overall energy efficiency for a wood gasification process targeting the production of synthetic natural gas (SNG) in SCWG is 70%. The overall energy efficiency is given in Equation (1) as:

$$\varepsilon = \frac{\Delta h^0_{SNG} \dot{m}^-_{SNG} + \dot{E}^- + \dot{Q}^-}{\Delta h^0_{biomass} \dot{m}^+_{biomass,daf} + \dot{E}^+} \quad (1)$$

where Δh_{SNG}^{0} refers to the lower heating value (LHV), $\dot{m}$ refers to the mass flow, $\dot{E}$ refers to the mechanical or electrical power, $\dot{Q}$ refers to the heat flow and *daf* refers to the dry ash free basis. The superscripts − and + refers to the flows leaving the system and flows entering the system, respectively. The same net efficiency for a SNG production process from wood were found to be 54.3% for an entrained flow gasifier operating at 3 MPa, 58.1% for a circulating fluidized bed operating at 1 MPa and 66.8% for an allothermal gasifier operating at 0.1 MPa on LHV basis [29].

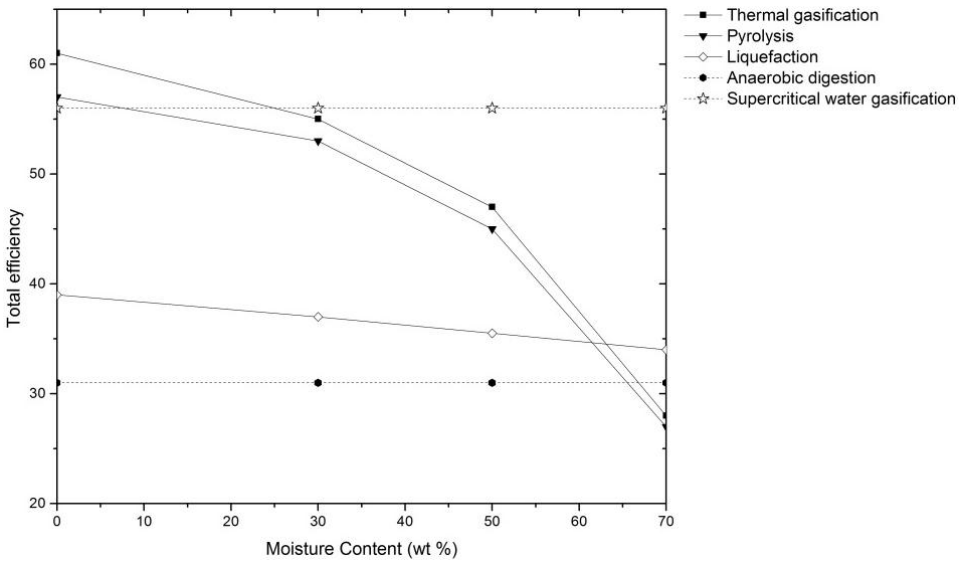

Figure 8. Total efficiency of heat utilization processes *versus* biomass moisture content; data taken from [30]. The total efficiency is defined as the HHV based energy content of the product divided by the energy content of all energy inputs to the process.

Supercritical water gasification of biomass can be performed under different process conditions with different feedstocks. The feedstock can be varied from simple model biomass compounds to complex real biomass feedstocks with or without the presence of catalyst at batch or continuous conditions. The experimental and modelling approaches of supercritical water gasification of biomass are described in detail in the next sections.

4. Supercritical Water Gasification of Biomass: Experimental Approaches

4.1. Understanding the Chemistry

Understanding the gasification reaction pathways of a real biomass is quite challenging due to the complex nature of a real biomass feedstock. However, performing experiments with representative model biomass compounds gives the opportunity to understand how the main ingredients of a real biomass could behave under the same process conditions. Cellulose, hemicellulose and lignin content of the biomass is generally represented by their monomers such as glucose, xylose and guaiacol, whereas the protein content of the biomass is represented by some major amino acids. Effects of inorganic content of the biomass are tested by performing model biomass experiments in the presence of some salt solutions.

4.1.1. Biopolymers

Cellulose conversion in supercritical water has been the subject of studies presented by Sasaki *et al.* [31,32] and Resende *et al.* [33]. The results show that cellulose undergoes a rapid hydrolysis and decomposes to its monomer glucose at very short residence times as short as 3 s at 400 °C. At higher temperatures, intermediate species formation starts and from these intermediates further gaseous compounds are formed. Real biomass derived hemicellulose conversion has not been investigated so far, however lignin conversion has been investigated by Yong and Matsumura [34,35] and Resende *et al.* [36]. The results show that lignin is mainly decomposed to guaiacol which further decomposes to other intermediates. These intermediates then form permanent gas products at higher temperatures. Char can be formed directly from lignin or through these intermediates.

4.1.2. Monomers

Glucose has been the main research focus among the other model biomass derived sugar compounds. The earliest research has been conducted by Amin *et al.* [6] in 1975. Lee *et al.* [37], Hao *et al.* [38], Williams and Onwudili [39], Goodwin and Rorrer [40], and Güngören Madenoğlu *et al.* [41] all performed parametric studies on the gasification of glucose in supercritical water. As expected, the increase in the temperature and residence time resulted in increased glucose conversion to gaseous products enhancing hydrogen production at higher temperatures.

Kabyemela *et al.* [42] and Matsumura *et al.* [43] examined the glucose decomposition pathways in supercritical water. They have proposed reaction pathways and determined the reaction rate constants for various temperatures. Kabyemela *et al.* [42] proposed that glucose undergoes an isomerization reaction to form fructose and then forms intermediates such as acids and 5-Hydroxymethylfurfural (5-HMF) at a temperature interval of 300–400 °C in which the decomposition reactions are proposed to be first order reactions. The intermediate products are proposed to be further converted to gas products at higher temperatures or longer residence times by different authors such as Goodwin and Rorrer [40] and Chuntanapum and Matsumura [44]. The latter research group proposed a general reaction mechanism for glucose to gas conversion. The reaction pathway is given in Figure 9. Similar to these researchers, Kruse and Gawlik [45] proposed that decomposition of glucose or fructose to furfurals is preferred under ionic conditions (characterized by a temperature lower than 374 °C), whereas a reaction pathway to acids or aldehydes is preferred at free radical conditions (characterized by temperatures higher than 374 °C).

Unlike glucose, there are only limited research works on the xylose reactions in supercritical water. Aida *et al.* [46] examined the xylose decomposition reactions at temperatures between 350 and 400 °C and Goodwin and Rorrer [47] examined its conversion at temperatures in the range of 450–650 °C. Similar to glucose reactions, xylose undergoes isomerization and decomposition reactions. The smaller organic compounds then further decompose to produce gas compounds at temperatures higher than 400 °C. Figure 10 shows the reaction mechanism of xylose in supercritical water within a temperature interval of 450 and 650 °C proposed by Goodwin and Rorrer [47].

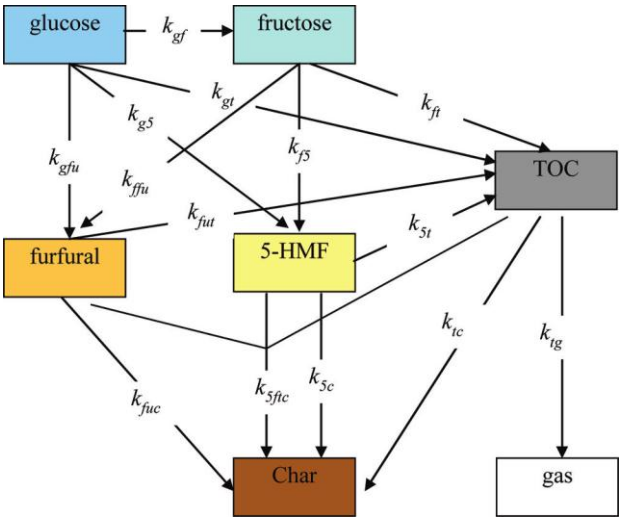

Figure 9. Proposed reaction pathway for glucose to gas conversion at temperatures between 300 and 400 ℃. Reprinted with permission from [44], copyright 2010 American Chemical Society. Please note that TOC refers to total organic compounds in liquid phase such as acids.

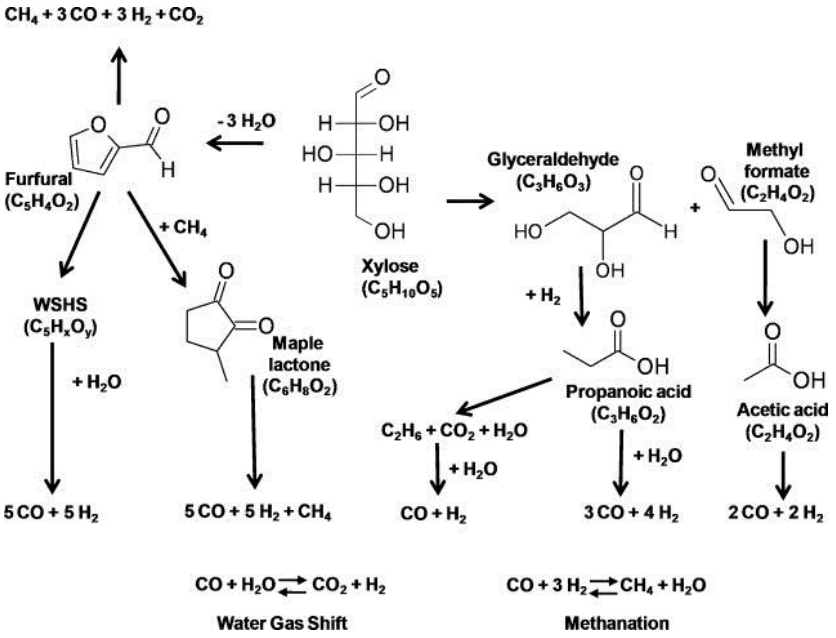

Figure 10. The reaction mechanism of xylose in supercritical water at a temperature interval of 450 and 650 ℃ proposed by Goodwin and Rorrer [47]. Reprinted with permission from [47], copyright 2010 Elsevier. WSHS refers to water soluble humic substances.

As a lignin model component, guaiacol conversion in supercritical water has been examined by Wahyudiono *et al.* [48,49] and Dileo *et al.* [50]. In addition, Yong and Matsumura [34,35] investigated the lignin decomposition pathway through guaiacol. The results indicate that guaiacol first decomposes to o-cresol, catechol, phenol and other liquid products. These intermediates further decompose to smaller compounds which then subsequently decompose to form gases. Figure 11 shows the lignin and guaiacol reaction mechanism at supercritical water at temperatures between 390 and 450 ℃. The reaction rates are assumed to be first order.

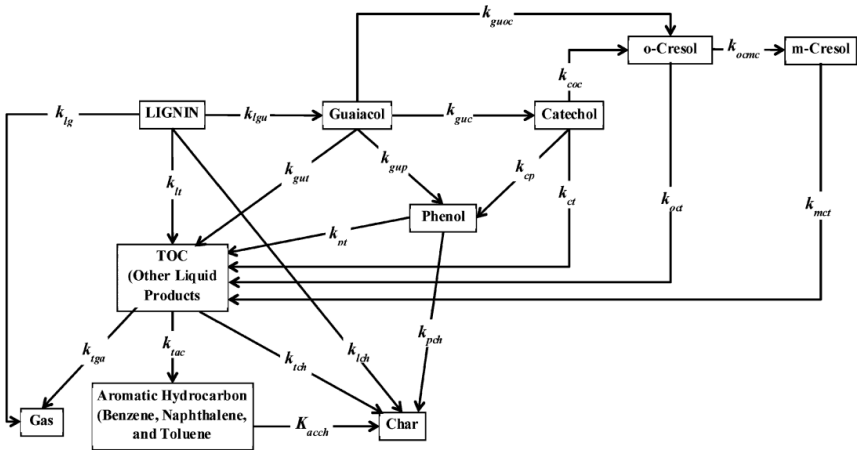

Figure 11. Lignin conversion and guaiacol reaction mechanism in supercritical water at temperatures between 390 and 450 °C as proposed by Yong and Matsumura [35]. Reprinted with permission from [35], copyright 2012 American Chemical Society. Yong and Matsumura [34] further proposed that aromatic hydrocarbons can be directly formed from lignin within the temperature range of 300–370 °C.

4.1.3. Amino Acids

Klingler *et al.* [51] examined the decomposition of two amino acids in sub- and supercritical water: alanine and glycine. The investigated temperature range was between 250 and 450 °C. The results indicate that both of the amino acids hydrolyze and release NH_3 to form acid intermediates as well as amine compounds. The acid compounds further decompose to produce smaller intermediates and gases. Figure 12 shows the reaction mechanism of amino acids in supercritical water proposed by the group. However, Dileo *et al.* [52] also observed solid, black product in addition to liquids and gases at 500 °C.

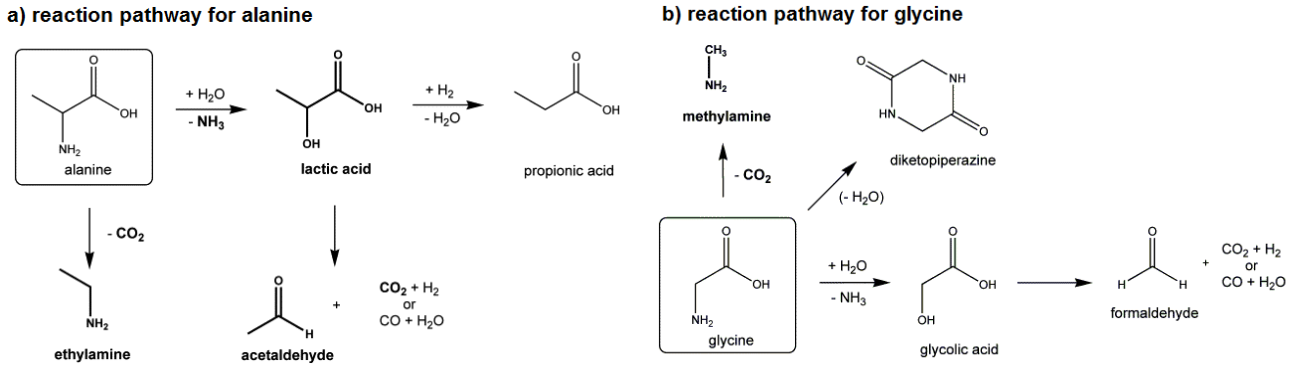

Figure 12. The reaction mechanism of (**a**) amino acids alanine and (**b**) glycine in supercritical water at 250–450 °C proposed by Klingler *et al.* [51]. Reprinted.

4.1.4. Intermediates

The conversion of intermediates in supercritical water has also been investigated by many researchers. Zhang *et al.* [53] and Shin *et al.* [54] examined the decomposition of formic acid in supercritical water. The results point to a mechanism in which formic acid undergoes dehydration and decarboxylation reactions to form carbon monoxide and carbon dioxide. Aida *et al.* [55] and Mok *et al.* [56] studied the

decomposition of lactic acid in supercritical water. The results are similar to formic acid reactions: lactic acid also undergoes dehydration and decarboxylation reactions and forms smaller intermediates such as acetaldehyde and acrylic acid. These intermediates further decompose to form gases. Chuntanapum and Matsumura [44,57,58] investigated the behavior of 5-HMF and its importance in char formation mechanism in supercritical water gasification reactions. Their results indicate that 5-HMF can undergo polymerization reactions and form char only at subcritical conditions. The pathway for 5-HMF is depicted in Figure 9.

4.1.5. Mixtures

In order to understand how real biomass could behave in gasification reactions, mixtures of two or more model biomass compounds have been investigated. Yoshida and Matsumura [59] investigated the gasification performance of mixtures of cellulose, xylan and lignin at 400 °C. They have proposed a correlation to predict the gasification and hydrogen production efficiency based on the amount of cellulose, xylan and lignin. The results indicate that the presence of lignin decreases the gas production as well as the production of H_2 from the intermediates of cellulose and xylan. Yoshida *et al.* [60] further investigated the gasification performance of sawdust and rice straw. They have compared the gasification efficiency and hydrogen production with their correlation. Gasification and hydrogen production yields were lower than those calculated values which led the authors to suggest that even in real biomass, interactions between each component occurred. Similar results have been observed by other authors: Weiss-Hortala *et al.* [61] observed a significant decrease in gas yields even when a small portion of phenol (a lignin decomposition compound) was blended with glucose. Goodwin and Rorrer [62] could not attain a 100% carbon gasification efficiency for xylose and phenol mixtures even at 750 °C. However, Castello and Fiori [63] reported that at 400 °C, phenol did not appear to behave as an inert compound, but contributed to gas production to a limited extent and reacted in liquid phase to form other compounds, possibly tar and/or solids.

4.1.6. Effect of Salts and the Role as Homogeneous Catalysts

The effect of inorganic constituents in biomass was investigated by gasifying model biomass compounds in the presence of salts. Sinag *et al.* [64] investigated the influence of K_2CO_3 on the gasification of glucose. Similarly, Kruse and Faquir [65] and Kruse *et al.* [66] tested the influence of other potassium containing alkali compounds such as KOH and $KHCO_3$. The authors found that the presence of alkali salts increases the total gas yield as well as hydrogen yield and the amount of phenols. Sinag *et al.* [64] proposed a reaction pathway for hydrogen formation in the presence of K_2CO_3 as:

$$K_2CO_3 + H_2O \rightarrow KHCO_3 + KOH \quad (2)$$

$$KOH + CO \rightarrow HCOOK \quad (3)$$

$$HCOOK + H_2O \rightarrow KHCO_3 + H_2 \quad (4)$$

$$2KHCO_3 \rightarrow H_2O + K_2CO_3 + CO_2 \quad (5)$$

$$H_2O + CO \leftrightarrow HCOOH \leftrightarrow H_2 + CO_2 \quad (6)$$

The positive effects of other (earth) alkali salts such as (NaOH, $Ca(OH)_2$, Na_2CO_3, $NaHCO_3$) on the gasification yield have also been reported by other authors [67–71] for different kinds of biomass feedstocks. Yildiz Bircan *et al.* [72] investigated the addition of $Ca(OH)_2$ on the gasification performance of an amino acid, L-cysteine. The results showed that the addition of $Ca(OH)_2$ enhanced the H_2 formation, but most importantly, it was observed that $Ca(OH)_2$ was consumed throughout the reactions and reacted with CO_2 to form $CaCO_3$.

4.1.7. Effect of Heterogeneous Catalysts

Catalysts are used in order to achieve higher conversion at lower temperatures (<500 °C), especially when the desired product is methane [73,74]. The presence of a catalyst changes the reaction pathway of the biomass, resulting in the reduction of tar and coke production and an increase in the gas yields. Figure 13 shows the influence of catalyst on the reaction pathway of wood gasification under supercritical conditions. Ruthenium, nickel and activated carbon based heterogeneous catalysts have been widely used in the literature [75–79] for both model and real biomass experiments enabling full carbon gasification efficiency to be obtained even at temperatures around 400 °C.

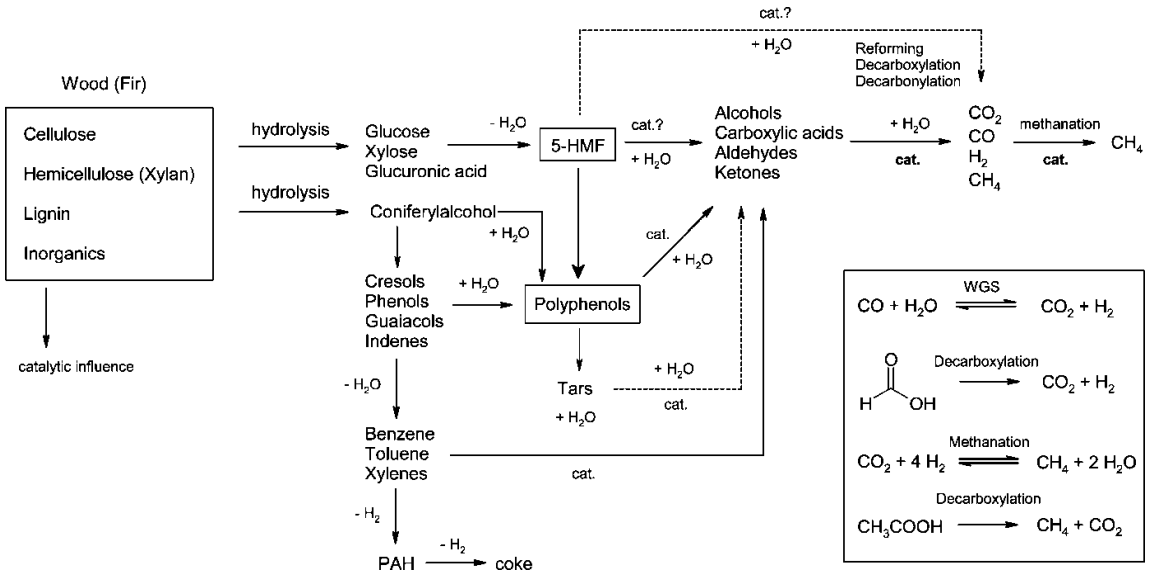

Figure 13. The influence of catalyst on the reaction pathway of wood gasification under supercritical conditions proposed by Waldner and Vogel [78]. Reprinted with permission from [78], copyright 2005 American Chemical Society. The term "cat." designates reaction pathways influenced by the presence of a catalyst, whereas the term "cat.?" denotes pathways that are only assumed to be promoted by a catalyst.

Yanik *et al.* [80] have investigated natural minerals like red mud (a by-product from alumina production plant containing Fe_2O_3 (37.7%), Al_2O_3 (17.3%), SiO_2 (17.1%), TiO_2 (4.8%), Na_2O (7.1%) and CaO (4.5%) by wt%) and trona ($NaHCO_3 \cdot Na_2CO_3 \cdot 2H_2O$). Both of these minerals have been found to significantly increase the H_2 yield and slightly promote the total gas yield for different kinds of carbohydrate based feedstocks.

It has been reported that the reactor wall material may also behave like a heterogeneous catalyst. Boukis *et al.* [81] studied the methanol reforming in a nickel-based alloy Inconel 625. They concluded

that the conversion rate as well as the product gas composition is influenced by the presence of heavy metals on the inner surface of the reactor and the catalytic effect remained high even after more than a thousand operation hours. Similarly, Gadhe and Gupta [82] observed a catalytic effect of the wall material from Inconel 600, which is an alloy of Ni, Cr and Fe, for methanol reforming. Lee *et al.* [37] performed glucose gasification in a reactor made of Hastelloy C-276 and noted a catalytic effect and enhancement in the hydrogen yields. Similar results were observed by Yu *et al.* [83]; these authors tested Inconel, new Hastelloy and corroded Hastelloy for glucose hydrothermal gasification. Their results indicated that corroded Hastelloy significantly increased the hydrogen and total gas yields. Castello *et al.* [84] have investigated the effect of wall material for stainless steel and Inconel 625 for both glucose and sawdust gasification in micro-autoclaves without the presence of catalyst at temperatures of 350 ℃ and 400 ℃. They have observed that stainless steel favored hydrogen production, whereas Inconel 625 enhanced CO consuming methanation and light hydrocarbon formation under supercritical conditions. Under subcritical conditions, the two reactors gave similar results.

4.1.8. Behavior of Heteroatoms

Yildiz Bircan *et al.* [72] investigated the behavior of heteroatoms such as S, N and P in supercritical water gasification using L-cysteine containing hetero-atoms S and N, and O-phospho-DL-serine containing P as feedstocks. They have performed experiments in an oven which was kept at 400 ℃ and at 26–27 MPa. After a residence time of 50 min, the oven was cooled to 30 ℃ and the components were analyzed. The results showed that sulphur partitioned to SO_2 and H_2S in the gas phase, and SO_3^{2-}, SO_4^{2-} and S^{2-} ions in the liquid phase. When $Ca(OH)_2$ was used as an additive, the gas phase sulphur compounds concentrations decreased by about one tenth and partitioned to the liquid phase sulphur. However, for both of the cases more than 90% of the sulphur partitioned to the solid phase. For nitrogen compounds, NO and NO_2 were detected in trace levels and NH_3 was not detectable. A total of 95.7% percent of nitrogen was converted to NH_4^+ in the liquid phase. This proportion decreased to 82% when $Ca(OH)_2$ was used as an additive. When it comes to phosphorus compounds, 93.3% of the phosphorus partitioned to ionic compounds in the liquid phase. When $Ca(OH)_2$ was used as an additive, more than 90% of the phosphorus precipitated as a solid phase.

4.1.9. Gas Phase Reactions

It has been reported by many authors (such as [47,85,86]) that water gas shift and methanation reactions are assumed to be the main gas phase reactions which may result in an equilibrium state. Equations (7) and (8) show the water gas shift reaction and methanation reactions, respectively.

$$CO + H_2O \leftrightarrow CO_2 + H_2 \quad (7)$$

$$CO + 3H_2 \leftrightarrow CH_4 + H_2O \quad (8)$$

In the water gas shift reaction, carbon monoxide and water form formic acid which further decomposes to carbon dioxide and hydrogen through the Equations (9) and (10) [87,88].

$$CO + H_2O \leftrightarrow HCOOH \quad (9)$$

$$HCOOH \leftrightarrow CO_2 + H_2 \quad (10)$$

Savage's group [85,86] performed sensitivity analyses on the reaction rates for non-catalytic supercritical water gasification of biomass processes. It can be concluded from the results that the main reactions which determine the hydrogen and methane formation are not the water gas shift and methanation reactions in the gas phase, but the reactions which directly result in the gas formation from the feedstock and/or intermediates. It has also been reported in the literature [87–90] that the rates of non-catalytic water gas shift and methanation reactions in supercritical water are quite slow, resulting in only 5% conversion even after several minutes.

4.2. Real Biomass Experiments

Antal *et al.* [75] state that the first real biomass experiments in supercritical water have been performed by Modell *et al.* [91] in 1985 using maple wood sawdust as a feedstock. The results indicated that the sawdust quickly decomposed to tars and gases without the formation of char. Since the first experiments in 1985, real biomass has also been the subject of supercritical water gasification.

4.2.1. Carbohydrates

In their work, Antal *et al.* [75] examined gasification performance of different biomass feedstocks such as corn- and potato-starch gels, wood sawdust suspended in a cornstarch gel, and potato wastes in three different tubular reactor which had activated carbon as a catalyst. They have performed experiments at temperatures higher than 650 °C and at a pressure of 28 MPa. Their results were in a good agreement with the equilibrium calculations resulting in an extraordinary gas yield higher than 2 L/g (liters of gas under 25 °C and 0.1 MPa per gram of organic matter in the feed) with a high yield of hydrogen (57%). Irrespective of the reactor geometry and method of heating, they have observed plugging problems after 1–2 h of operation time with feedstocks that contained approximately 15 wt% of organic material.

D'Jesús *et al.* [92] gasified corn starch, clover grass and corn silage in supercritical water. They investigated the influence of pressure, temperature, residence time and alkali addition on gasification performance. They reported that the change in the pressure did not alter the gasification yield; however, the increase in the temperature significantly increased the gasification yield. Longer residence time resulted in higher gasification yields till the system attained a maximum. Potassium addition (in the form of $KHCO_3$) was found to increase the carbon gasification efficiency for corn starch. Although, no significant difference was observed for clover grass and corn silage as they naturally contained potassium.

4.2.2. Algae

Stucki *et al.* [93] gasified a microalgae species, *Spirulina platensis*, in the presence of different catalysts. One hundred percent of the carbon content of the microalgae was gasified using a Ru/C catalysts at a temperature of around 400 °C and at a pressure around 32 MPa. Their results were in very good agreement with the equilibrium predictions. They proposed that 60%–70% of the heating value of the algae can be recovered in the form of methane.

Chakinala *et al.* [94] gasified *Chlorella Vulgaris* in supercritical water. They have observed more than 80% carbon gasification efficiency at 700 °C with a 7.3 wt% dry mass concentration at a pressure

of 24 MPa with a residence time of 2 min. As expected, gasification efficiency decreased with a decrease in temperature and residence time. The increase in the dry mass concentration had a negative impact on the carbon gasification efficiency. They have also tested the effect of different catalysts on the carbon gasification efficiency. The results indicated that the presence of a catalyst increased the carbon gasification efficiency, reaching even a 100% with a Ru/TiO_2 catalyst at 600 °C with a residence time of 2 min.

Guan *et al.* [95] gasified another microalgae sample, *Nannochloropsis* sp., in supercritical water at 450–550 °C at around 25 MPa. They have concluded that higher gas yields were obtained by higher temperatures, longer reaction times (>20 min), higher water densities, and lower algae loadings. Their findings also show that when the biomass loading reduced from 15 wt% to 1 wt%, H_2 yield more than tripled.

Onwudili *et al.* [71] gasified three different types of microalgae samples (*Chlorella vulgaris*, *Spirulina platensis* and *Saccharina latissima*) at 500 °C and 36 MPa in an Inconel batch reactor for 30 min. They also tested the influence of NaOH and/or $Ni\text{-}Al_2O_3$ on the gasification performance. Their results indicated that the presence of NaOH more than doubled the hydrogen yield and decreased the tar yield up to 71%. Presence of the nickel catalyst had also decreased the tar formation. A similar study has been performed by Bagnoud-Velásquez *et al.* [96] on the effluent recycling and the catalytic gasification of a microalgae sample, *Phaeodactylum tricornutum*. In a continuous reactor, for a 6.5 wt% algae concentration, they were able to obtain 31% carbon gasification efficiency at 420 °C and 32.3 MPa in the presence of Ru/C catalysts. They observed rapid deactivation of the catalyst due to sulphur poisoning and coke formation.

4.2.3. Sludge

Xu and Antal [97] gasified digested sewage sludge, corn starch and poplar wood sawdust in the presence of coconut shell activated carbon catalyst. They have mixed sewage sludge (up to 7.69 wt%) with corn starch gel (up to 7.69 wt%) in order to form a viscous gel. They have performed experiments at 650 °C and at 28 MPa. Even with a lower sewage sludge loading (2.1 dry wt% digested sewage sludge with dry 5.1 wt% corn starch), the reactor had plugging problems after 1–2 h of operation time due to high ash content of sewage sludge.

Chen *et al.* [98] used a fluidized bed to overcome reactor plugging problems in sewage sludge gasification. They have also tested the effect of operating parameters as temperature, concentration of the feedstock, alkali catalysts and catalyst loading on gaseous products and carbon distribution. The authors have performed experiments at a pressure of 25 MPa and at a temperature range of 480–540 °C with a biomass concentration varying from 4 to 12 wt%. As expected, the increase in temperature and decrease in feed concentration increased the carbon gasification efficiency. Addition of alkali catalyst was found to enhance the hydrogen production.

Zhai *et al.* [99] gasified digested sewage sludge in a batch reactor at temperatures up to 425 °C at a pressure varying from 25 to 35 MPa, with a residence time of 10–15 min and a dry matter content ranging from 5 to 25 wt%. In the best case, they were able to obtain 3.5% carbon gasification efficiency where the presence of K_2CO_3 increased this value up to 26%.

4.2.4. Manure

Waldner [13] gasified real biomass samples such as wood and swine manure in a batch reactor in the presence of different catalysts. Using a Raney Ni 2800 catalyst, 100% carbon gasification efficiency was obtained at a temperature around 400 °C and at a pressure of 31 MPa for wood. The gas composition was in agreement with the equilibrium predictions. Similar conditions resulted in more than 75% carbon gasification efficiency for swine manure.

Nakamura *et al.* [77] investigated the gasification of chicken manure in the presence of suspended fine activated carbon catalysts in an experimental pilot plant. At 600 °C and 25 MPa with a residence time of 1.7 min, they were able to completely gasify 2 wt% and 10 wt% chicken manure in the presence of 0.4 wt% and 5 wt% activated carbon, respectively. However, when there was no catalyst present, 80% carbon gasification efficiency was observed with a 2 wt% feed concentration. Their setup included a liquefaction process with a residence time of 26.7 min of which the temperature was 180 °C and pressure was 1.2 MPa.

Yong and Matsumura [100] investigated the gasification behavior of poultry manure and eucalyptus wood in a flow reactor and the effect of activated carbon on the gasification performance. Their results indicate that addition of 0.1 wt% wood to 0.5 wt% manure increased the carbon gasification efficiency (CGE) at temperatures between 550 and 650 °C and at a pressure of 25 MPa. However, the effect of wood decreased at 0.2 wt% and became almost insignificant at 0.3 wt%. They stated that cellulose and hemicellulose containing wood biomass are more easily decomposed in SCW than poultry manure. The increase in the loading of wood in the mixture resulted in the deceleration of the gas producing pathways in the overall reactions. It was also found that the usage of activated carbon in the feedstock mixture improved the gasification efficiency. An overview of the real biomass experiments is presented in Table 1.

Table 1. An overview of the real biomass experiments.

Feedstock	wt%	Temperature (°C)	Pressure (MPa)	Reactor type	Residence time	CGE (%)	Mole fraction of gas products (%)				Reference
							CH_4	CO_2	H_2	CO	
Corn Starch	10.4	~700	28	Tubular with a carbon catalyst	2.18 h	91	22	38	37	2	[75]
Microalgae (*Chlorella Vulgaris*)	7.3	600	24	Quartz Capillary	2 min	53	25	26	7	22	[94]
Sewage Sludge	10	540	25	Fluidized Bed	N/A	32	13	43	26	13.5	[98]
Swine Manure	13.2	405	30.1	Batch reactor with nickel catalyst	36 min	75.8	46	43	10.7	0.1	[13]
Chicken Manure	10	600	25	Flow reactor with carbon catalyst	1.7 min	90	21.2	45.4	28.7	0	[77]

5. Supercritical Water Gasification of Biomass: Modeling Approaches

Modeling enables simulating real cases in order to predict products and equipment performances and overcome possible challenges for different process conditions.

5.1. Kinetic Modeling

Studies aimed at elucidating the reaction kinetics under hydrothermal gasification conditions have started with simple sugar compounds and have been extended later to real biomass feedstocks. Matsumura's group [43,44,57,58] and Kabyemela *et al.* [42] studied the glucose, fructose and glucose derived intermediate decompositions in sub- and supercritical water. Aida *et al.* [46] and Goodwin and Rorrer [47] investigated the reactions of D-xylose in sub- and supercritical water. Wahyudiono *et al.* [49] studied the thermal decomposition kinetics of guaiacol as a lignin derived material. Sasaki *et al.* [31,101] further studied the kinetics of cellulose and cellobiose conversion in sub- and supercritical water. Regarding modelling, Resende and Savage [86] developed a kinetic model for non-catalytic supercritical water gasification of cellulose and lignin at high temperatures, and Guan *et al.* [85] proposed a reaction mechanism for the supercritical water gasification of a real biomass feedstock; microalgae. However, these kinetic models and parameters have limited applicability as:

- in most of these works, all of the reactions are assumed to be first order reactions;
- the temperature effect on the rate constants has not been sufficiently investigated;
- most of these works only incorporate the decomposition rates and the formation of intermediates, but do not show the whole gasification routes;
- the models which include entire gasification routes incorporate the lumped kinetic model, which neglects the composition of intermediates.

Another interesting approach to kinetic modeling is the detailed kinetic modeling. Here, the whole reaction mechanisms consist of hundreds of elementary reactions. Most of these attempts have been made for SCWO of simple compounds such as methanol, carbon monoxide, methane and hydrogen [18,102–106]. Detailed kinetic modeling has also been applied for supercritical water gasification systems. Ederer *et al.* [107] have investigated the pyrolysis of tert-butylbenzene in supercritical water, Bühler *et al.* [108] investigated the glycerol decomposition in supercritical water and Castello and Fiori [109] used the detailed kinetic models for the supercritical water oxidation of methanol to model the gasification of methanol in supercritical water. Even though the results are promising, the application of detailed kinetic modeling for real biomass is not viable yet due to the complex nature of real biomass feedstocks. Table 2 shows an overview of the kinetic parameters for the selected conversion pathways of biomass constituent compounds during supercritical water gasification.

Table 2. An overview of the kinetic parameters determined for selected conversion pathways of biomass constituent compounds during supercritical water gasification. Please note that TOC refers to water-soluble organic species such as 1,2,4-benzenetriol, 1,4-benzenediol, 5-methyl-2-furaldehyde, levulinic acid, and formic acid.

Compound	Type of Reaction	Activation Energy (kJ mol^{-1})	Pre-Exp. Factor (s^{-1})	Temperature Range (℃)	Pressure (Mpa)	Reference
Cellulose	Conversion	145.9	$1 \times 10^{11.9}$	320–370	25	[31]
Cellulose	Conversion	547.9	$1 \times 10^{44.6}$	370–400	25	[31]
Cellobiose	Conversion	96.4	1.28×10^{8}	300–350	25	[110]
Cellobiose	Conversion	96.4	1.48×10^{8}	350–400	30	[110]
Cellobiose	Hydrolysis	108.6	1.10×10^{9}	300–350	25	[110]
Cellobiose	Hydrolysis	108.6	1.15×10^{9}	350–400	30	[110]
Cellobiose	Pyrolysis to glucosyl-eryhtrose and glycoaldehyde	30.4	17.68	300–350	25	[110]
Cellobiose	Pyrolysis to glucosyl-eryhtrose and glycoaldehyde	30.4	57.13	350–400	30	[110]
Cellobiose	Pyrolysis to glucosyl-glycoaldehyde and eryhtrose	69.3	82,730.74	300–350	25	[110]
Cellobiose	Pyrolysis to glucosyl-glycoaldehyde and eryhtrose	69.3	83,456.10	350–400	30	[110]
Glucose	Decomposition	121	1.33×10^{10}	175–400	25	[43]
Glucose	Decomposition	96	1.23×10^{8}	300–350	25	[111]
Glucose	Isomerization to fructose	112.75	2.99×10^{9}	300–400	25–30	[42]
Fructose	Decomposition to acids	130.94	7.48×10^{10}	300–400	25–30	[42]
Glucose	Conversion to 5-HMF	114.40	1.49×10^{8}	300–400	25	[44]
Glucose	Conversion to non-furfural organics	137.40	2.05×10^{11}	300–400	25	[44]
TOC	Conversion to gas products	27.92	0.78	300–400	25	[44]
TOC	Conversion to char	17.29	0.04	300–400	25	[44]
Xylose	Conversion to furfural	120.1	1.20×10^{12}	450–650	25	[47]
Furfural	Conversion to WSHS	55.6	5.70×10^{3}	450–650	25	[47]
WSHS	Conversion to gas	138.9	1.60×10^{8}	450–650	25	[47]
Guaiacol	Conversion	40.0	1.87×10^{3}	380–400	30	[48]

5.2. Computational Fluid Dynamics Modeling

Computational fluid dynamics (CFD) modeling helps to simulate and design a reactor [112]. Yoshida and Matsumura [112] were the first researchers who performed CFD analysis for a SCWG reactor. The authors used Fluent 6.3® software to perform simulations for 4.9 wt% glucose conversion in the presence of hydrogen peroxide as oxidation agent in supercritical water at 400 ℃ and 25.4 MPa. However, the authors ignored all the reactions and calculated only the flow of water and inert particles as virtual char products.

Goodwin and Rorrer [113] performed CFD simulations for xylose gasification in a Hastelloy micro-channel reactor at 650 ℃ and 25 MPa. The authors used Fluent 6.3.26® for the simulations and the fluid was modeled by the Navier-Stokes equations for laminar flow. They performed simulations using a six-reaction based kinetic model which they developed in a previous paper [47]. The authors used Peng-Robinson EoS for the pure gas species for the calculation of the fugacities; however, the mixing interactions in the reacting fluid were taken into account. The authors found that CFD simulations accurately predicted the gas yields. Besides, it was found that the endothermic xylose gasification reactions had little influence on the reaction temperature, thus not affecting the gas yield or H_2 selectivity.

Wei *et al.* [114] performed CFD simulations with a Eulerian model which incorporates the mechanical kinetic theory for solid particles to predict the solid distribution and the residence time distribution of the feeding materials for a fluidized bed reactor. Based on the simulation results, they proposed a feeding pipe with an angle of 45 ° to enable a uniform solid distribution and long residence time among the reactor.

A different approach using CFD has been performed by Withag *et al.* [115,116]. Here, the authors performed CFD simulations to calculate heat transfer characteristics of supercritical water to a flow reactor for both 1D and 2D cases. Further, Withag [117] also performed simulations for a reacting flow of methanol in supercritical water for a 2D case. Based on the simulations, it was concluded that methanol is mainly converted near the wall due to the high fluid temperatures resulting in high local reaction rates.

5.3. Thermodynamic Equilibrium Modeling

In addition to the kinetic models, supercritical water gasification of biomass compounds has also been modelled following a thermodynamic equilibrium modelling approach. Antal *et al.* [75] were the first researchers who used the thermodynamic equilibrium approach. They compared the experimental results with the thermodynamic equilibrium predictions using STANJAN and HYSIM of which the first one uses ideal gas assumption as an equation of state (EoS) and the latter one Peng–Robinson EoS. Tang and Kitagawa [118] performed thermodynamic analysis for various model and real biomass compounds using Peng-Robinson EoS describing the non-ideal properties of the compounds. The authors used a Gibbs free energy minimization method (also known as the non-stoichiometric method) in order to predict the equilibrium amounts of gases. More authors followed the same approach [119–124]. All of these works have been developed for the supercritical region and take only the gas phase compounds into account. Castello and Fiori [125] extended the gas phase products and introduced graphitic carbon as an additional compound, and investigated the application of thermodynamic constraints such as solid carbon formation and process heat duty.

An alternative to Gibbs free energy minimization was given in the works of Letellier *et al.* [126] and Marias *et al.* [127]. Here, the authors used the discrete reaction equilibria method (also known as stoichiometric approach) to predict the equilibrium composition of the gas phase compounds. Furthermore, they also modeled the flash column for the separation of product gases from water and other organic compounds.

The aforementioned developed models do not cover the subcritical region of the process and the behavior of inorganics, and the partitioning behavior of elements. However, Yanagida *et al.* [79]

investigated the equilibrium behavior of inorganic elements in poultry manure during supercritical water gasification using a software; HSC Chemistry 6.12. Seven inorganic elements, namely N, Ca, K, P, S, Cl and Si, as well as C, H, O content of manure and possible compounds that could be formed by these elements, have been taken into account for the thermodynamic equilibrium calculations. The simulation was run first at 32 MPa and 600 °C and, after subtracting the amount of gases formed, the simulation then was run at room temperature conditions to observe the phase and compound behavior of the elements. The results have been compared with experimental works and found to be in agreement. A similar approach has been conducted by Yakaboylu *et al.* [12]. Here, the authors used the software packages of FactSage 5.4.1 and SimuSage 1.12 for the prediction of the equilibrium partitioning of 12 elements on the basis of compounds and phases for a mixture of pig and cow manure sample. The simulations have been performed for a wide range of temperatures (100–580 °C), pressures (25–30 MPa) and dry mass concentrations (5–20 wt%). The same research group [128] has also developed a multi-phase thermodynamic model for the prediction of equilibrium state compounds for supercritical water gasification of biomass systems. The authors validated the model by comparing their predictions with experimental results and model predictions already published. They also performed a case study for a microalgae sample and investigated the behavior of gaseous compounds and elements at different pressures and temperatures as well as dry matter concentrations. Table 3 shows an overview of the thermodynamic equilibrium modeling papers. There are other research works in the literature which use commercial software packages for the prediction of product compounds following a thermodynamic equilibrium calculation approach. However, most of these works concentrate on process modeling which is discussed in detail in the following section.

Table 3. An overview of the thermodynamic equilibrium modeling of supercritical water gasification of biomass papers.

Investigated compounds	Type of approach	Type of EoS or software used for the calculations	Considered phases	Significant contribution	Reference
Methanol, glucose, cellulose, starch, sawdust	Gibbs free energy minimization (GFEM)	Peng-Robinson EoS	Only gas phase	The first paper with a thermodynamic model	[118]
Glucose	GFEM	Duan EoS	Only gas phase	The introduction of additional constraints	[124]
Wood sawdust	GFEM	Duan EoS	Gas phase and solid carbon	The introduction of solid carbon	[122]
Poultry manure	GFEM	HSC chemistry 6.12	Multi-Phase	The first paper which took the inorganic elements into account	[79]
Methanol, ethanol, glycerol, glucose and cellulose	GFEM	Ideal gas	Gas phase and solid carbon	No need for initial guesses for the mole amount of product species	[123]
Methanol, glucose, sewage sludge	Reaction equilibria	Peng-Robinson EoS	Gas phase and solid carbon	The first paper which used the reaction equilibria method	[126]

Table 3. *Cont.*

Investigated compounds	Type of approach	Type of EoS or software used for the calculations	Considered phases	Significant contribution	Reference
Glycerol and microalgae	GFEM	Peng-Robinson EoS	Gas phase and solid carbon	Char formation conditions have been examined	[125]
Glucose and cellulose	GFEM	Virial EoS and ideal gas	Only gas phase	Introduction of the entropy maximization	[120]
Pig-Cow manure mix	GFEM	FactSage 5.4.1 and SimuSage 1.12	Multi-Phase	The first paper which investigated the partitioning behavior of elements	[12]
Microalgae	GFEM	Peng-Robinson EoS for gases and revised HKF EoS for the aqueous compounds	Multi-Phase	The first paper which proposed a multi-phase mathematical model for both subcritical and supercritical regions	[128]

It is a fact that an arbitrary multi-component multi-phase system at a given temperature, pressure and chemical composition will always tend to minimize its total Gibbs free energy till it reaches the global minimum state. However, the predicted compounds at that minimum state are the "unconstrained" equilibrium state compounds. Most of the real conversion systems do not reach that state due to the natural constraints (such as slow kinetics or reaction barrier conditions) that could keep the system away from it [129]. In that sense, for most of the cases, predictions using a thermodynamic equilibrium approach will not show the real case results but will give an insight in the process limits as well as the formation behavior of the compounds.

5.4. Process Modeling

Even though thermodynamic equilibrium models predict the (major) product compounds formed in reactors, one needs to model the performance of the other equipment in such a biomass based supercritical water gasification processing plant in order to gain insight into the whole process performance. Feng *et al.* [130] were the first researchers who performed a thermodynamic analysis of a supercritical water biomass gasification plant. They have analyzed the phase behavior and phase equilibria in the reactor and separators; in addition, they designed an optimized heat exchange network and performed a system exergy analysis. The authors used the statistical association fluids theory (SAFT) EoS for the thermodynamic calculations. Their results indicated that a cellulose gasification plant with reactor operating conditions of 600 ℃ and 35 MPa has an exergy efficiency of 40.6%. The exergy efficiency in this work is defined as the ratio of the exergy flows of the inlet (cellulose as being the feedstock, providing heat and electricity for the process) and outlet (hydrogen-rich) products.

Luterbacher *et al.* [131] performed process simulations and life cycle assessment (LCA) for wood and manure as a feedstock in supercritical water gasification plant targeting to produce SNG. Using AspenPlus^{TM} 2004.1 software for the process simulations, their results showed that 62% of the manure's

lower heating value (LHV) is converted to SNG and 71% of wood's LHV is converted to SNG. Similarly, Gassner *et al.* [28,132] offered optimal process design for polygeneration of SNG, power and heat from various biomass sources varying from a typical lignocellulosic material (modeled as $CH_{1.35}O_{0.63}$) to manure and sewage sludge. The authors made an extensive analysis from both thermo-economic and optimization points of view concerning the processes. The results indicate that the SNG conversion efficiency of wood process was found to reach up to 70%. The same value was found to reach up to 75% for microalgae, 70% for manure and 60% for undigested sewage sludge where the SNG conversion efficiency is given in Equation (11) as:

$$\varepsilon = \frac{\Delta h^0_{SNG} \dot{m}^-_{SNG}}{\Delta h^0_{biomass} \dot{m}^+_{biomass,daf}} \quad (11)$$

where Δh^0_{SNG} refers to the LHV, $\dot{m}$ refers to the mass flow and *daf* refers to the dry ash free basis. The superscripts − and + refer to the flows leaving the system and flows entering the system, respectively.

Gutiérrez Ortiz *et al.* [133] performed process simulations using AspenPlus™ for gasification of glycerol in supercritical water. They investigated the effect of process conditions on the hydrogen yield. Using predictive Soave-Redlich-Kwong EoS for Gibbs free energy minimization in the reactor to predict the equilibrium composition, the authors concluded that the highest yield for hydrogen could be obtained at 900 °C with 1 mol % glycerol in the feed. The authors reported that the pressure did not have an influence on the results.

A similar research has been conducted by Fiori *et al.* [134]. The authors performed process simulations using AspenPlus™ aiming at hydrogen production and energetic self-sustainability of different biomass feedstocks of glycerol, phenol, microalgae *Spirulina*, sewage sludge and grape marc. Their results indicated that biomass feed share should be at a minimum of 15–25 wt% in order to establish an energetic self-sustainable process (11.4 wt% for phenol and 22.9 wt% for *Spirulina* for a reactor operating at 700 °C and 30 MPa). The results also indicate that the thermal energy required for the microalgae process is around 0.6 MJ (kg-total-feed)$^{-1}$ for a reactor operating at 500 °C and 30 MPa when the dry biomass concentration in the feed is 10 wt%. This value is around 1.5 MJ (kg-total-feed)$^{-1}$ for a reactor operating at 700 °C with the same process conditions.

Another process simulation concerning a system model based on methanol gasification has been performed by Withag *et al.* [135]. Here, the authors also used AspenPlus™ and tested the validity of different EoS concluding that the property methods based on the Peng–Robinson and Soave Redlich-Kwong EoS all give a prediction of the H_2 mole fraction within a bandwidth of 3.5% compared to experimental results. They have also performed simulations for different cases to predict the thermal efficiencies for methanol, glucose and cellulose conversion. Similar to the findings of Fiori *et al.* [134], the authors concluded that the dry mass concentration of the feed should be at least 14.5 wt% for methanol and ~25 wt% for cellulose and glucose to have a thermal efficiency of 60% for a reactor operating at 600 °C and 30 MPa.

6. Process Challenges and Reactor Technology Aspects for Industrial Applications

Most of the experiments have been conducted in batch reactors which are not suitable for industrial applications. In contrast, industry rather demands continuous processes. However, continuous experimental

approaches have some challenges which need to be overcome in order to scale up the process and be applicable in industry.

Pumpability of the biomass slurry is a problem in continuous processes. The dry matter content of the biomass slurry should not exceed the pumpability limits due to possible clogging problems. On the other hand, a high dry matter content results in higher gas production which increases the energy efficiency and the profitability of the plant. Yet, the pumpability of the biomass slurry depends on the nature of the biomass [136]. Antal *et al.* [75] used a cement pump to be able to pump a suspension of 4 wt% starch gel mixed with wood sawdust and other particulate biomass. On the other hand, sewage sludge containing 40% dry matter can be successfully pumped [137]. A pretreatment of reducing the particle size of the biomass [136] and obtaining a suspended feed [75] can be used to overcome the possible pumpability problems.

Corrosion is another problem for industrial scale applications. The process takes place in harsh conditions which lead to corrosion of the reactor construction material. In addition, gases and minerals which are formed during the gasification lead to corrosion as well [136]. Marrone and Hong [138] propose some corrosion control approaches which are (i) vortex/circulating flow reactor to prevent corrosive species from reaching a solid surface; (ii) use of high corrosion resistant materials such as nickel based alloys or stainless steel or (iii) reducing the temperature to 400 °C instead of 600 °C to improve the energy balance which would enable using other types of corrosion control methods such as using liners or coatings that decrease the heat transfer.

Working at low temperatures might have a positive effect on solving corrosion and energy efficiency problems, however, carbon gasification efficiency decreases due to the slower reaction rates. One way to overcome such problems is to use catalysts to enhance the reaction rates. Waldner and Vogel [78] have already obtained a full carbon gasification for wood samples and sufficiently high carbon efficiency (>80%) for swine manure experiments at low temperatures (~400 °C) using catalysts. Similar results have been observed by other researchers [93] as well. However, in addition to increasing the process costs—catalysts are often reported to be prone to deactivation problems [73,139–141] caused by (i) the poisoning of the active surface of the catalyst by sulfur; (ii) fouling of the catalyst surface by precipitated salts and other minerals and (iii) coke formation and deposition on the catalyst surface [142]. Coke formation may also cause plugging problems in flow reactors [143].

Zöhrer *et al.* [144] state that mixing the unheated, relatively concentrated organic solution with the preheated water avoids unwanted reactions and coke formation caused by the slow heating of the organic feed. However, this option could be feasible only for model biomass compounds as the concentrated biomass slurry would not be suitable for pumping as discussed earlier. For real biomass processes, rapid heating of the feed can overcome such coke and tar formation behavior as the positive effect of rapid heating on less tar production and higher gas yields are reported by other researchers [145,146] as well. Another possible solution to coke and tar formation was given by Kruse and Faquir [65]. The authors proposed a reaction process in which a continuously stirred tank reactor (CSTR) is followed by a tubular reactor in order to benefit from the "active hydrogen" formation in the CSTR due to its backmixing. "Active hydrogen", which is referred as the *in statu nascendi* hydrogen formed through the intermediate stages of the water gas shift reaction or by hydrogen, is reported to suppress tar and coke formation reactions. Furthermore, the gas yields increases when the CSTR is combined with a tubular reactor.

Obtaining sufficient process thermal efficiency is another challenge for supercritical water gasification of biomass systems. Thermal efficiency should be high enough to make the process viable for industrial applications. The efficiency becomes more important when the desired reactor temperature increases [136]. Proposed process demonstration units [73] as well as the VERENA pilot plant in Karlsruhe Institute of Technology [147,148] benefit from the high temperature of the product stream leaving from the reactor in order to preheat the feed using a heat exchanger. However, as reported earlier, if the heating rate of the heat exchanger is low, coke and tar formation will take place. To overcome such problems, VERENA pilot plant mixes the concentrated biomass, which was heated up to the critical temperature, with high temperature pure water [147]. The process flow diagram of VERENA pilot plant is given in Figure 14. Another approach was given by researchers in State Key Laboratory of Multiphase Flow in Power Engineering (SKLMF) of China [149–152]. Here, the researchers proposed solar energy based heating for the reactor and successfully applied this energy source for supercritical water gasification of biomass compounds. The Dutch company Gensos B.V. has patented a process that incorporates extensive heat recovery which enables a high process thermal efficiency [153].

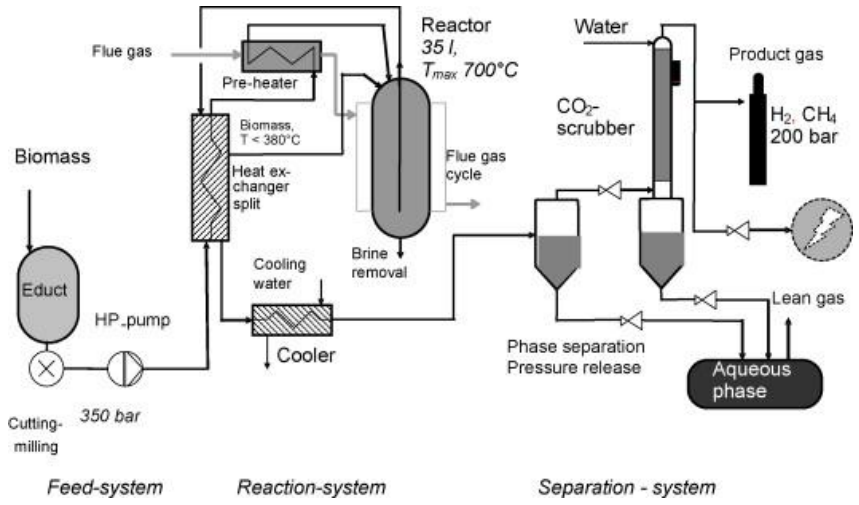

Figure 14. The process flow diagram of VERENA pilot plant. Reprinted with permission from [136], copyright 2009 Elsevier.

The most important challenge in supercritical water gasification of biomass processes remains the salt precipitation due to the rapid decrease in the solubility of salts in the supercritical region (see Figure 5). The precipitated salts may lead to plugging problems if the tube diameters are small, crystals are large or sticky, heterogeneous catalysts are used, and the velocity of the flow is low [136]. The first possible solutions to salt precipitation problem were offered in the 1980s [154] and 1990s [155,156] as the salt precipitation was also a major problem for supercritical water oxidation processes. Hong *et al.* [154] patented a reverse flow reactor (known as MODAR reactor) in which the feedstock is fed from the top of the reactor and the cold water from the bottom. The upper part of the reactor is kept at supercritical temperatures, whereas the bottom part is kept at subcritical temperatures. Supercritical fluid leaves the reactor from the top and a brine effluent leaves from the bottom. Daman [155,156] patented a transpiring wall reactor in which solute-free water flows through a porous reactor liner in order to keep salt deposition as well as corrosion problems away from the reactor wall [157]. Xu *et al.* [158] combined these two approaches for a sewage sludge supercritical water oxidation process which is expected to

prevent reactor plugging and corrosion problems. However, Marrone and Hong [138] stated that the transpiring wall reactor has limited usefulness for gasification systems due to adverse effect of dilution on the system's energy balance. On the other hand, Schubert *et al.* [159] used a salt separation vessel which the design is similar to MODAR's reverse flow reactor. The feed inlet and effluent to the reactor are from the top, whereas the brine effluent is from the bottom. The top of the reactor is at supercritical and the bottom part is at subcritical temperatures. In contrast to MODAR reactor which acts as both salt separator and reactor, salt separation vessel proposed by Schubert *et al.* [159] is a kind of pretreatment unit before the reactor. Zöhrer *et al.* [141] used this salt separator to perform catalytic gasification and liquefaction of fermentation residue samples. They observed almost no salt separation at 430 °C. At 450 °C, the salt separation efficiency was higher. However, at 470 °C massive tar formation which led to blockage in the rig was observed. Similar to MODAR reactor, Boukis *et al.* [147,148] used a reactor in the VERENA pilot plant which acts as both reactor and salt separator. The lower part of the reactor has a cooler [160] that enables the brines and solids leaving the reactor via a third output from the lower part of the reactor.

Another possible solution for plugging problems in the reactor was proposed by Matsumura and Minowa [5]. The authors speculated on the potential benefits of applying a fluidized bed reactor to the supercritical water gasification process. They investigated the fundamental design parameters of such a fluidized bed. Potic *et al.* [161] performed fluidization experiments for supercritical water in micro cylindrical quartz reactor with an internal diameter of 1 mm. Lu *et al.* [162] were the first researchers who performed supercritical water gasification experiments in a fluidized bed reactor at SKLMF. The reactor material was constructed from 316 mm stainless steel. The bed diameter was 30 mm, freeboard diameter was 40 mm, and the total length was 915 mm. The authors stated that no reactor plugging was observed. Other researchers in SKLMF [98,163] continued to perform gasification experiments in the same fluidized bed reactor. Real biomass experiments (2 wt% sewage sludge + 2 wt% sodium carboxymethyl cellulose) resulted in more than 40% carbon gasification efficiency at a temperature of 540 °C and at a pressure of 25 MPa. Gensos B.V. has patented a process and apparatus that incorporates a fluidized bed reactor [164,165].

7. Conclusions

Supercritical water gasification is a promising technology for the efficient conversion of wet biomass into a product gas that after upgrading can be used as substitute natural gas or hydrogen rich gas. The gasification behavior and the chemistry of the decomposition reactions of the model biomass compounds have been well examined throughout the decades; this work made a survey of mechanisms proposed and associated reaction kinetics. Thermodynamic modeling has been performed by several groups with quite some success and an overview of these attempts was given in this paper. Attempts have also been made for real biomass feedstocks varying from manure to sewage sludge. The results show the great potential of using supercritical water for gasification purposes. However, the process still faces some challenges which need to be overcome in order to enter the market. The main challenges seem to be thermal efficiency, plugging and corrosion problems. Fortunately, new reactor technologies and process concepts are being developed for the aforementioned problems.

Acknowledgments

This research project is carried out within the Agentschap NL funded project "Superkritische vergassing van natte reststromen" (contract EOSLT10051). The authors would like to thank to Güçhan Yapar for his help in the preparation of Table 2.

Authors Contributions

Please prepare a short, one paragraph statement giving the individual contribution of each co-author to the reported research and writing of the paper.

Conflicts of Interest

The authors declare no conflict of interest.

References

1. *U.S. Energy Information Administration International Energy Outlook 2013*; Report Number: DOE/EIA-0484(2013); U.S. Department of Energy: Washington, DC, USA, 2013.
2. Process: The potential for biomass in the energy mix. *Filtr. Sep.* **2006**, *43*, 28–30.
3. Basu, P.; Mettanant, V. Biomass gasification in supercritical water—a review. *Int. J. Chem. React. Eng.* **2009**, *7*, 1–61.
4. *European Commission Biomass—Green Energy for Europe*; Report Number: EUR21350; European Commission: Brussels, Belgium, 2005.
5. Matsumura, Y.; Minowa, T. Fundamental design of a continuous biomass gasification process using a supercritical water fluidized bed. *Int. J. Hydrog. Energy* **2004**, *29*, 701–707.
6. Amin, S.; Reid, R.; Modell, M. Reforming and decomposition of glucose in an aqueous phase. In Proceedings of the Intersociety Conference on Environmental Systems, San Francisco, CA, USA, 21–24 July 1975.
7. Barner, H.E.; Huang, C.Y.; Johnson, T.; Jacobs, G.; Martch, M.A.; Killilea, W.R. Supercritical water oxidation: An emerging technology. *J. Hazard. Mater.* **1992**, *31*, 1–17.
8. Brunner, G. Near critical and supercritical water. Part I. Hydrolytic and hydrothermal processes. *J. Supercrit. Fluids* **2009**, *47*, 373–381.
9. Peterson, A.A.; Vogel, F.; Lachance, R.P.; Fröling, M.; Antal, M.J.J.; Tester, J.W. Thermochemical biofuel production in hydrothermal media: A review of sub- and supercritical water technologies. *Energy Environ. Sci.* **2008**, *1*, 32–65.
10. Kruse, A.; Dinjus, E. Hot compressed water as reaction medium and reactant: Properties and synthesis reactions. *J. Supercrit. Fluids* **2007**, *39*, 362–380.
11. Wagner, W.; Pruß, A. The IAPWS formulation 1995 for the thermodynamic properties of ordinary water substance for general and scientific use. *J. Phys. Chem. Ref. Data* **2002**, *31*, 387–535.
12. Yakaboylu, O.; Harinck, J.; Gerton Smit, K.G.; de Jong, W. Supercritical water gasification of manure: A thermodynamic equilibrium modeling approach. *Biomass Bioenergy* **2013**, *59*, 253–263.

13. Waldner, M.H. Catalytic Hydrothermal Gasification of Biomass for the Production of Synthetic Natural Gas. Ph.D. Thesis, Eidgenössische Technische Hochschule/Paul Scherrer Institute: Zürich, Switzerland, 2007.
14. Masaru Watanabe, T.S. Chemical reactions of C(1) compounds in near-critical and supercritical water. *Chem. Rev.* **2004**, *104*, 5803–5821.
15. Armellini, F.J. Phase Equilibria and Precipitation Phenomena of Sodium Chloride and Sodium Sulfate in Sub- and Supercritical Water. Ph.D. Thesis, Massachusetts Institute of Technology, Cambridge, MA, USA, 1993.
16. Connolly, J.F. Solubility of hydrocarbons in water near the critical solution temperatures. *J. Chem. Eng. Data* **1966**, *11*, 13–16.
17. Marshall, W.L.; Franck, E.U. Ion product of water substance, 0–1000 °C, 1–10,000 bars New International Formulation and its background. *J. Phys. Chem. Ref. Data* **1981**, *10*, doi:10.1063/1.555643.
18. Webley, P.A.; Tester, J.W. Fundamental kinetics of methane oxidation in supercritical water. *Energy Fuels* **1991**, *5*, 411–419.
19. Thermophysical Properties of Fluid Systems. Available online: http://webbook.nist.gov/chemistry/fluid/ (accessed on 6 June 2014).
20. Castello, D. Supercritical Water Gasification of Biomass. Ph.D. Thesis, University of Trento, Trento, Italy, 2013.
21. Coronella, C.J.; Lynam, J.G.; Reza, M.T.; Uddin, M.H. Hydrothermal carbonization of lignocellulosic biomass. In *Application of Hydrothermal Reactions to Biomass Conversion*; Jin, F., Ed.; Springer: Berlin, Germany, 2014; pp. 275–311.
22. Onwudili, J.A. Hydrothermal gasification of biomass for hydrogen production. In *Application of Hydrothermal Reactions to Biomass Conversion*; Jin, F., Ed.; Springer: Berlin, Germany, 2014; pp. 219–246.
23. Toor, S.S.; Rosendahl, L.A.; Hoffmann, J.; Pedersen, T.H.; Nielsen, R.P.; Søgaard, E.G. Hydrothermal liquefaction of biomass. In *Application of Hydrothermal Reactions to Biomass Conversion*; Jin, F., Ed.; Springer: Berlin, Germany, 2014; pp. 189–217.
24. Xu, C.C.; Shao, Y.; Yuan, Z.; Cheng, S.; Feng, S.; Nazari, L.; Tymchyshyn, M. Hydrothermal Liquefaction of Biomass in Hot-Compressed Water, Alcohols, and Alcohol-Water Co-solvents for Biocrude Production. In *Application of Hydrothermal Reactions to Biomass Conversion*; Jin, F., Ed.; Springer: Berlin, Germany, 2014; pp. 171–187.
25. Bermejo, M.D.; Cocero, M.J. Supercritical water oxidation: A technical review. *AIChE J.* **2006**, *52*, 3933–3951.
26. Hodes, M.; Marrone, P.A.; Hong, G.T.; Smith, K.A.; Tester, J.W. Salt precipitation and scale control in supercritical water oxidation—Part A: Fundamentals and research. *J. Supercrit. Fluids* **2004**, *29*, 265–288.
27. Cortright, R.D.; Davda, R.R.; Dumesic, J.A. Hydrogen from catalytic reforming of biomass-derived hydrocarbons in liquid water. *Nature* **2002**, *418*, 964–967.
28. Gassner, M.; Vogel, F.; Heyen, G.; Maréchal, F. Optimal process design for the polygeneration of SNG, power and heat by hydrothermal gasification of waste biomass: Process optimisation for selected substrates. *Energy Environ. Sci.* **2011**, *4*, 1742–1758.

29. Van der Meijden, C.M.; Veringa, H.J.; Rabou, L.P.L.M. The production of synthetic natural gas (SNG): A comparison of three wood gasification systems for energy balance and overall efficiency. *Biomass Bioenergy* **2010**, *34*, 302–311.
30. Yoshida, Y.; Dowaki, K.; Matsumura, Y.; Matsuhashi, R.; Li, D.; Ishitani, H.; Komiyama, H. Comprehensive comparison of efficiency and CO_2 emissions between biomass energy conversion technologies—Position of supercritical water gasification in biomass technologies. *Biomass Bioenergy* **2003**, *25*, 257–272.
31. Sasaki, M.; Adschiri, T.; Arai, K. Kinetics of cellulose conversion at 25 MPa in sub- and supercritical water. *AIChE J.* **2004**, *50*, 192–202.
32. Sasaki, M.; Kabyemela, B.; Malaluan, R.; Hirose, S.; Takeda, N.; Adschiri, T.; Arai, K. Cellulose hydrolysis in subcritical and supercritical water. *J. Supercrit. Fluids* **1998**, *13*, 261–268.
33. Resende, F.L.P.; Neff, M.E.; Savage, P.E. Noncatalytic gasification of cellulose in supercritical water. *Energy Fuels* **2007**, *21*, 3637–3643.
34. Yong, T.L.-K.; Matsumura, Y. Kinetic analysis of lignin hydrothermal conversion in sub- and supercritical Water. *Ind. Eng. Chem. Res.* **2013**, *52*, 5626–5639.
35. Yong, T.L.-K.; Matsumura, Y. Reaction kinetics of the lignin conversion in supercritical water. *Ind. Eng. Chem. Res.* **2012**, *51*, 11975–11988.
36. Resende, F.L.P.; Fraley, S.A.; Berger, M.J.; Savage, P.E. Noncatalytic gasification of lignin in supercritical water. *Energy Fuels* **2008**, *22*, 1328–1334.
37. Lee, I.-G.; Kim, M.-S.; Ihm, S.-K. Gasification of glucose in supercritical water. *Ind. Eng. Chem. Res.* **2002**, *41*, 1182–1188.
38. Hao, X.H.; Guo, L.J.; Mao, X.; Zhang, X.M.; Chen, X.J. Hydrogen production from glucose used as a model compound of biomass gasified in supercritical water. *Int. J. Hydrog. Energy* **2003**, *28*, 55–64.
39. Williams, P.T.; Onwudili, J. Composition of products from the supercritical water gasification of glucose: A model biomass compound. *Ind. Eng. Chem. Res.* **2005**, *44*, 8739–8749.
40. Goodwin, A.K.; Rorrer, G.L. Conversion of glucose to hydrogen-rich gas by supercritical water in a microchannel reactor. *Ind. Eng. Chem. Res.* **2008**, *47*, 4106–4114.
41. Güngören Madenoğlu, T.; Sağlam, M.; Yüksel, M.; Ballice, L. Simultaneous effect of temperature and pressure on catalytic hydrothermal gasification of glucose. *J. Supercrit. Fluids* **2013**, *73*, 151–160.
42. Kabyemela, B.M.; Adschiri, T.; Malaluan, R.M.; Arai, K. Glucose and fructose decomposition in subcritical and supercritical water: Detailed reaction pathway, mechanisms, and kinetics. *Ind. Eng. Chem. Res.* **1999**, *38*, 2888–2895.
43. Matsumura, Y.; Yanachi, S.; Yoshida, T. Glucose decomposition kinetics in water at 25 MPa in the temperature range of 448–673 K. *Ind. Eng. Chem. Res.* **2006**, *45*, 1875–1879.
44. Chuntanapum, A.; Matsumura, Y. Char formation mechanism in supercritical water gasification process: A study of model compounds. *Ind. Eng. Chem. Res.* **2010**, *49*, 4055–4062.
45. Kruse, A.; Gawlik, A. Biomass conversion in water at 330–410 ℃ and 30–50 MPa. Identification of key compounds for indicating different chemical reaction pathways. *Ind. Eng. Chem. Res.* **2003**, *42*, 267–279.

46. Aida, T.M.; Shiraishi, N.; Kubo, M.; Watanabe, M.; Smith, R.L. Reaction kinetics of D-xylose in sub- and supercritical water. *J. Supercrit. Fluids* **2010**, *55*, 208–216.
47. Goodwin, A.K.; Rorrer, G.L. Reaction rates for supercritical water gasification of xylose in a micro-tubular reactor. *Chem. Eng. J.* **2010**, *163*, 10–21.
48. Wahyudiono, W; Kanetake, T.; Sasaki, M.; Goto, M. Decomposition of a lignin model compound under hydrothermal conditions. *Chem. Eng. Technol.* **2007**, *30*, 1113–1122.
49. Wahyudiono, W; Sasaki, M.; Goto, M. Thermal decomposition of guaiacol in sub- and supercritical water and its kinetic analysis. *J. Mater. Cycles Waste Manag.* **2011**, *13*, 68–79.
50. Dileo, G.J.; Neff, M.E.; Savage, P.E. Gasification of guaiacol and phenol in supercritical water. *Energy Fuels* **2007**, *21*, 2340–2345.
51. Klingler, D.; Berg, J.; Vogel, H. Hydrothermal reactions of alanine and glycine in sub- and supercritical water. *J. Supercrit. Fluids* **2007**, *43*, 112–119.
52. Dileo, G.J.; Neff, M.E.; Kim, S.; Savage, P.E. Supercritical water gasification of phenol and glycine as models for plant and protein biomass. *Energy Fuels* **2008**, *22*, 871–877.
53. Zhang, Y.; Zhang, J.; Zhao, L.; Sheng, C. Decomposition of formic acid in supercritical water. *Energy Fuels* **2010**, *24*, 95–99.
54. Shin, K.S.; Cho, H.Y.; Nam, Y.W.; Lee, D.S. Hydrothermal decomposition of formic acid in sub- and supercritical water. *Environ. Eng. Res.* **1998**, *3*, 61–66.
55. Aida, T.M.; Ikarashi, A.; Saito, Y.; Watanabe, M.; Smith, R.L.; Arai, K. Dehydration of lactic acid to acrylic acid in high temperature water at high pressures. *J. Supercrit. Fluids* **2009**, *50*, 257–264.
56. Mok, W.S.; Antal, M.J.; Jones, M. Formation of acrylic acid from lactic acid in supercritical water. *J. Org. Chem.* **1989**, *54*, 4596–4602.
57. Chuntanapum, A.; Matsumura, Y. Formation of tarry material from 5-HMF in subcritical and supercritical water. *Ind. Eng. Chem. Res.* **2009**, *48*, 9837–9846.
58. Chuntanapum, A.; Yong, T.L.-K.; Miyake, S.; Matsumura, Y. Behavior of 5-HMF in subcritical and supercritical water. *Ind. Eng. Chem. Res.* **2008**, *47*, 2956–2962.
59. Yoshida, T.; Matsumura, Y. Gasification of cellulose, xylan, and lignin mixtures in supercritical water. *Ind. Eng. Chem. Res.* **2001**, *40*, 5469–5474.
60. Yoshida, T.; Oshima, Y.; Matsumura, Y. Gasification of biomass model compounds and real biomass in supercritical water. *Biomass Bioenergy* **2004**, *26*, 71–78.
61. Weiss-Hortala, E.; Kruse, A.; Ceccarelli, C.; Barna, R. Influence of phenol on glucose degradation during supercritical water gasification. *J. Supercrit. Fluids* **2010**, *53*, 42–47.
62. Goodwin, A.K.; Rorrer, G.L. Conversion of xylose and xylose-phenol mixtures to hydrogen-rich gas by supercritical water in an isothermal microtube flow reactor. *Energy Fuels* **2009**, *23*, 3818–3825.
63. Castello, D.; Kruse, A.; Fiori, L. Supercritical water gasification of glucose/phenol mixtures as model compounds for ligno-cellulosic biomass. *Chem. Eng. Trans.* **2014**, *37*, 193–198.
64. Sınağ, A.; Kruse, A.; Schwarzkopf, V. Key compounds of the hydropyrolysis of glucose in supercritical water in the presence of K_2CO_3. *Ind. Eng. Chem. Res.* **2003**, *42*, 3516–3521.
65. Kruse, A.; Faquir, M. Hydrothermal biomass gasification—effects of salts, backmixing and their interaction. *Chem. Eng. Technol.* **2007**, *30*, 749–754.
66. Kruse, A.; Meier, D.; Rimbrecht, P.; Schacht, M. Gasification of pyrocatechol in supercritical water in the presence of potassium hydroxide. *Ind. Eng. Chem. Res.* **2000**, *39*, 4842–4848.

67. Guo, Y.; Wang, S.; Wang, Y.; Zhang, J.; Xu, D.; Gong, Y. Gasification of two and three-components mixture in supercritical water: Influence of NaOH and initial reactants of acetic acid and phenol. *Int. J. Hydrog. Energy* **2012**, *37*, 2278–2286.
68. Minowa, T.; Zhen, F.; Ogi, T. Cellulose decomposition in hot-compressed water with alkali or nickel catalyst. *J. Supercrit. Fluids* **1998**, *13*, 253–259.
69. Muangrat, R.; Onwudili, J.A.; Williams, P.T. Influence of alkali catalysts on the production of hydrogen-rich gas from the hydrothermal gasification of food processing waste. *Appl. Catal. B Environ.* **2010**, *100*, 440–449.
70. Muangrat, R.; Onwudili, J.A.; Williams, P.T. Alkali-promoted hydrothermal gasification of biomass food processing waste: A parametric study. *Int. J. Hydrog. Energy* **2010**, *35*, 7405–7415.
71. Onwudili, J.A.; Lea-Langton, A.R.; Ross, A.B.; Williams, P.T. Catalytic hydrothermal gasification of algae for hydrogen production: Composition of reaction products and potential for nutrient recycling. *Bioresour. Technol.* **2013**, *127*, 72–80.
72. Yildiz Bircan, S.; Kamoshita, H.; Kanamori, R.; Ishida, Y.; Matsumoto, K.; Hasegawa, Y.; Kitagawa, K. Behavior of heteroatom compounds in hydrothermal gasification of biowaste for hydrogen production. *Appl. Energy* **2011**, *88*, 4874–4878.
73. Matsumura, Y.; Minowa, T.; Potic, B.; Kersten, S.; Prins, W.; van Swaaij, W.; Vandebeld, B.; Elliott, D.; Neuenschwander, G.; Kruse, A.; *et al*. Biomass gasification in near- and super-critical water: Status and prospects. *Biomass Bioenergy* **2005**, *29*, 269–292.
74. Zöhrer, H. Hydrothermal gasification of fermentation residues for SNG-production. Ph.D. Thesis, Swiss Federal Institute of Technology in Zurich, Zürich, Switzerland, 2013.
75. Antal, M.J.; Allen, S.G.; Schulman, D.; Xu, X.; Divilio, R.J. Biomass gasification in supercritical water. *Ind. Eng. Chem. Res.* **2000**, *39*, 4040–4053.
76. Byrd, A.J.; Pant, K.K.; Gupta, R.B. Hydrogen production from glycerol by reforming in supercritical water over Ru/Al_2O_3 catalyst. *Fuel* **2008**, *87*, 2956–2960.
77. Nakamura, A.; Kiyonaga, E.; Yamamura, Y.; Shimizu, Y.; Minowa, T.; Noda, Y.; Matsumura, Y. Gasification of catalyst-suspended chicken manure in supercritical water. *J. Chem. Eng. Jpn.* **2008**, *41*, 433–440.
78. Waldner, M.H.; Vogel, F. Renewable production of methane from woody biomass by catalytic hydrothermal gasification. *Ind. Eng. Chem. Res.* **2005**, *44*, 4543–4551.
79. Yanagida, T.; Minowa, T.; Nakamura, A.; Matsumura, Y.; Noda, Y. Behavior of inorganic elements in poultry manure during supercritical water gasification. *J. Jpn. Inst. Energy* **2008**, *87*, 731–736.
80. Yanik, J.; Ebale, S.; Kruse, A.; Saglam, M.; Yüksel, M. Biomass gasification in supercritical water: II. Effect of catalyst. *Int. J. Hydrog. Energy* **2008**, *33*, 4520–4526.
81. Boukis, N.; Diem, V.; Habicht, W.; Dinjus, E. Methanol reforming in supercritical water. *Ind. Eng. Chem. Res.* **2003**, *42*, 728–735.
82. Gadhe, J.B.; Gupta, R.B. Hydrogen production by methanol reforming in supercritical water: Suppression of methane formation. *Ind. Eng. Chem. Res.* **2005**, *44*, 4577–4585.
83. Yu, D.; Aihara, M.; Antal, M.J. Hydrogen production by steam reforming glucose in supercritical water. *Energy Fuels* **1993**, *7*, 574–577.
84. Castello, D.; Kruse, A.; Fiori, L. Biomass gasification in supercritical and subcritical water: The effect of the reactor material. *Chem. Eng. J.* **2013**, *228*, 535–544.

85. Guan, Q.; Wei, C.; Savage, P.E. Kinetic model for supercritical water gasification of algae. *Phys. Chem. Chem. Phys.* **2012**, *14*, 3140–3147.
86. Resende, F.L.P.; Savage, P.E. Kinetic model for noncatalytic supercritical water gasification of cellulose and lignin. *AIChE J.* **2010**, *56*, 2412–2420.
87. Araki, K.; Fujiwara, H.; Sugimoto, K.; Oshima, Y.; Koda, S. Kinetics of water-gas shift reaction in supercritical water. *J. Chem. Eng. Jpn.* **2004**, *37*, 443–448.
88. Rice, S.F.; Steeper, R.R.; Aiken, J.D. Water density effects on homogeneous water-gas shift reaction kinetics. *J. Phys. Chem. A* **1998**, *102*, 2673–2678.
89. Sato, T.; Kurosawa, S.; Smith, R.L., Jr.; Adschiri, T.; Arai, K. Water gas shift reaction kinetics under noncatalytic conditions in supercritical water. *J. Supercrit. Fluids* **2004**, *29*, 113–119.
90. Kruse, A.; Dinjus, E. Hydrogen from methane and supercritical water. *Angew. Chem. Int. Ed.* **2003**, *42*, 909–911.
91. Modell, M. Gasification and liquefaction of forest products in supercritical water. In *Fundamentals of Thermochemical Biomass Conversion*; Overend, R., Milne, T., Mudge, L., Eds.; Elsevier: Amsterdam, The Netherlands, 1985; pp. 95–119.
92. D'Jesús, P.; Boukis, N.; Kraushaar-Czarnetzki, B.; Dinjus, E. Gasification of corn and clover grass in supercritical water. *Fuel* **2006**, *85*, 1032–1038.
93. Stucki, S.; Vogel, F.; Ludwig, C.; Haiduc, A.G.; Brandenberger, M. Catalytic gasification of algae in supercritical water for biofuel production and carbon capture. *Energy Environ. Sci.* **2009**, *2*, 535–541.
94. Chakinala, A.G.; Brilman, D.W.F.; van Swaaij, W.P.M.; Kersten, S.R.A. Catalytic and non-catalytic supercritical water gasification of microalgae and glycerol. *Ind. Eng. Chem. Res.* **2010**, *49*, 1113–1122.
95. Guan, Q.; Savage, P.E.; Wei, C. Gasification of alga Nannochloropsis sp. in supercritical water. *J. Supercrit. Fluids* **2012**, *61*, 139–145.
96. Bagnoud-Velásquez, M.; Brandenberger, M.; Vogel, F.; Ludwig, C. Continuous catalytic hydrothermal gasification of algal biomass and case study on toxicity of aluminum as a step toward effluents recycling. *Catal. Today* **2014**, *223*, 35–43.
97. Xu, X.; Antal, M.J. Gasification of sewage sludge and other biomass for hydrogen production in supercritical water. *Environ. Prog.* **1998**, *17*, 215–220.
98. Chen, Y.; Guo, L.; Cao, W.; Jin, H.; Guo, S.; Zhang, X. Hydrogen production by sewage sludge gasification in supercritical water with a fluidized bed reactor. *Int. J. Hydrog. Energy* **2013**, *38*, 12991–12999.
99. Zhai, Y.; Wang, C.; Chen, H.; Li, C.; Zeng, G.; Pang, D.; Lu, P. Digested sewage sludge gasification in supercritical water. *Waste Manag. Res.* **2013**, *31*, 393–400.
100. Yong, T.L.-K.; Matsumura, Y. Catalytic gasification of poultry manure and eucalyptus wood mixture in supercritical water. *Ind. Eng. Chem. Res.* **2012**, *51*, 5685–5690.
101. Sasaki, M.; Furukawa, M.; Minami, K.; Adschiri, T.; Arai, K. Kinetics and mechanism of cellobiose hydrolysis and retro-aldol condensation in subcritical and supercritical water. *Ind. Eng. Chem. Res.* **2002**, *41*, 6642–6649.
102. Brock, E.E.; Savage, P.E. Detailed chemical kinetics model for supercritical water oxidation of C_1 compounds and H_2. *AIChE J.* **1995**, *41*, 1874–1888.

103. Brock, E.E.; Savage, P.E.; Barker, J.R. A reduced mechanism for methanol oxidation in supercritical water. *Chem. Eng. Sci.* **1998**, *53*, 857–867.
104. Brock, E.E.; Oshima, Y.; Savage, P.E.; Barker, J.R. Kinetics and mechanism of methanol oxidation in supercritical water. *J. Phys. Chem.* **1996**, *100*, 15834–15842.
105. Helling, R.K.; Tester, J.W. Oxidation kinetics of carbon monoxide in supercritical water. *Energy Fuels* **1987**, *1*, 417–423.
106. Tester, J.W.; Webley, P.A.; Holgate, H.R. Revised global kinetic measurements of methanol oxidation in supercritical water. *Ind. Eng. Chem. Res.* **1993**, *32*, 236–239.
107. Ederer, H.J.; Kruse, A.; Mas, C.; Ebert, K.H. Modelling of the pyrolysis of tert-butylbenzene in supercritical water. *J. Supercrit. Fluids* **1999**, *15*, 191–204.
108. Bühler, W.; Dinjus, E.; Ederer, H.J.; Kruse, A.; Mas, C. Ionic reactions and pyrolysis of glycerol as competing reaction pathways in near- and supercritical water. *J. Supercrit. Fluids* **2002**, *22*, 37–53.
109. Castello, D.; Fiori, L. Kinetics modeling and main reaction schemes for the supercritical water gasification of methanol. *J. Supercrit. Fluids* **2012**, *69*, 64–74.
110. Kabyemela, B.M.; Takigawa, M.; Adschiri, T.; Malaluan, R.M.; Arai, K. Mechanism and Kinetics of Cellobiose Decomposition in Sub- and Supercritical Water. *Ind. Eng. Chem. Res.* **1998**, *37*, 357–361.
111. Kabyemela, B.M.; Adschiri, T.; Malaluan, R.M.; Arai, K. Kinetics of glucose epimerization and decomposition in subcritical and supercritical water. *Ind. Eng. Chem. Res.* **1997**, *36*, 1552–1558.
112. Yoshida, T.; Matsumura, Y. Reactor development for supercritical water gasification of 4.9 wt% glucose solution at 673 K by using computational fluid dynamics. *Ind. Eng. Chem. Res.* **2009**, *48*, 8381–8386.
113. Goodwin, A.K.; Rorrer, G.L. Modeling of supercritical water gasification of xylose to hydrogen-rich gas in a hastelloy microchannel reactor. *Ind. Eng. Chem. Res.* **2011**, *50*, 7172–7182.
114. Wei, L.; Lu, Y.; Wei, J. Hydrogen production by supercritical water gasification of biomass: Particle and residence time distribution in fluidized bed reactor. *Int. J. Hydrog. Energy* **2013**, *38*, 13117–13124.
115. Withag, J.A.M.; Sallevelt, J.L.H.P.; Brilman, D.W.F.; Bramer, E.A.; Brem, G. Heat transfer characteristics of supercritical water in a tube: Application for 2D and an experimental validation. *J. Supercrit. Fluids* **2012**, *70*, 156–170.
116. Sallevelt, J.L.H.P.; Withag, J.A.M.; Bramer, E.A.; Brilman, D.W.F.; Brem, G. One-dimensional model for heat transfer to a supercritical water flow in a tube. *J. Supercrit. Fluids* **2012**, *68*, 1–12.
117. Withag, J.A.M. On the Gasification of Wet Biomass in Supercritical Water. Ph.D. Thesis, University of Twente, Enschede, The Netherlands, 2013.
118. Tang, H.; Kitagawa, K. Supercritical water gasification of biomass: Thermodynamic analysis with direct Gibbs free energy minimization. *Chem. Eng. J.* **2005**, *106*, 261–267.
119. Freitas, A.C.; Guirardello, R. Thermodynamic analysis of supercritical water gasification of microalgae biomass for hydrogen and syngas production. *Chem. Eng. Trans.* **2013**, *32*, 553–558.
120. Freitas, A.C.D.; Guirardello, R. Supercritical water gasification of glucose and cellulose for hydrogen and syngas production. *Chem. Eng. Trans.* **2012**, *27*, 361–366.

121. Freitas, A.C.D.; Guirardello, R. Comparison of several glycerol reforming methods for hydrogen and syngas production using Gibbs energy minimization. *Int. J. Hydrog. Energy* **2014**, *39*, 17969–17984.
122. Lu, Y.; Guo, L.; Zhang, X.; Yan, Q. Thermodynamic modeling and analysis of biomass gasification for hydrogen production in supercritical water. *Chem. Eng. J.* **2007**, *131*, 233–244.
123. Voll, F.A.P.; Rossi, C.C.R.S.; Silva, C.; Guirardello, R.; Souza, R.O.M.A.; Cabral, V.F.; Cardozo-Filho, L. Thermodynamic analysis of supercritical water gasification of methanol, ethanol, glycerol, glucose and cellulose. *Int. J. Hydrog. Energy* **2009**, *34*, 9737–9744.
124. Yan, Q.; Guo, L.; Lu, Y. Thermodynamic analysis of hydrogen production from biomass gasification in supercritical water. *Energy Convers. Manag.* **2006**, *47*, 1515–1528.
125. Castello, D.; Fiori, L. Supercritical water gasification of biomass: Thermodynamic constraints. *Bioresour. Technol.* **2011**, *102*, 7574–7582.
126. Letellier, S.; Marias, F.; Cezac, P.; Serin, J.P. Gasification of aqueous biomass in supercritical water: A thermodynamic equilibrium analysis. *J. Supercrit. Fluids* **2010**, *51*, 353–361.
127. Marias, F.; Letellier, S.; Cezac, P.; Serin, J.P. Energetic analysis of gasification of aqueous biomass in supercritical water. *Biomass Bioenergy* **2011**, *35*, 59–73.
128. Yakaboylu, O.; Harinck, J.; Smit, K.G.; de Jong, W. Supercritical water gasification of biomass: A thermodynamic model for the prediction of product compounds at equilibrium state. *Energy Fuels* **2014**, *28*, 2506–2522.
129. Kozeschnik, E. A numerical model for evaluation of unconstrained and compositionally constrained thermodynamic equilibria. *Calphad* **2000**, *24*, 245–252.
130. Feng, W.; van der Kooi, H.J.; de Swaan Arons, J. Biomass conversions in subcritical and supercritical water: Driving force, phase equilibria, and thermodynamic analysis. *Chem. Eng. Process. Process Intensif.* **2004**, *43*, 1459–1467.
131. Luterbacher, J.S.; Fröling, M.; Vogel, F.; Maréchal, F.; Tester, J.W. Hydrothermal gasification of waste biomass: Process design and life cycle asessment. *Environ. Sci. Technol.* **2009**, *43*, 1578–1583.
132. Gassner, M.; Vogel, F.; Heyen, G.; Maréchal, F. Optimal process design for the polygeneration of SNG, power and heat by hydrothermal gasification of waste biomass: Thermo-economic process modelling and integration. *Energy Environ. Sci.* **2011**, *4*, 1726–1741.
133. Gutiérrez Ortiz, F.J.; Ollero, P.; Serrera, A.; Sanz, A. Thermodynamic study of the supercritical water reforming of glycerol. *Int. J. Hydrog. Energy* **2011**, *36*, 8994–9013.
134. Fiori, L.; Valbusa, M.; Castello, D. Supercritical water gasification of biomass for H_2 production: Process design. *Bioresour. Technol.* **2012**, *121*, 139–147.
135. Withag, J.A.M.; Smeets, J.R.; Bramer, E.A.; Brem, G. System model for gasification of biomass model compounds in supercritical water—A thermodynamic analysis. *J. Supercrit. Fluids* **2012**, *61*, 157–166.
136. Kruse, A. Hydrothermal biomass gasification. *J. Supercrit. Fluids* **2009**, *47*, 391–399.
137. Tolman, R. *Process for Converting Sewage Sludge and Municipal Solid Wastes to Clean Fuels*; Report Number: P600-01-12; California Energy Commission: Sacramento, CA, USA, 2001.
138. Marrone, P.A.; Hong, G.T. Corrosion control methods in supercritical water oxidation and gasification processes. *J. Supercrit. Fluids* **2009**, *51*, 83–103.

139. Elliott, D.C. Catalytic hydrothermal gasification of biomass. *Biofuels Bioprod. Biorefin.* **2008**, *2*, 254–265.
140. Guo, Y.; Wang, S.Z.; Xu, D.H.; Gong, Y.M.; Ma, H.H.; Tang, X.Y. Review of catalytic supercritical water gasification for hydrogen production from biomass. *Renew. Sustain. Energy Rev.* **2010**, *14*, 334–343.
141. Zöhrer, H.; de Boni, E.; Vogel, F. Hydrothermal processing of fermentation residues in a continuous multistage rig—Operational challenges for liquefaction, salt separation, and catalytic gasification. *Biomass Bioenergy* **2014**, *65*, 51–63.
142. Zöhrer, H.; Vogel, F. Hydrothermal catalytic gasification of fermentation residues from a biogas plant. *Biomass Bioenergy* **2013**, *53*, 138–148.
143. Karayıldırım, T.; Sınağ, A.; Kruse, A. Char and Coke Formation as Unwanted Side Reaction of the Hydrothermal Biomass Gasification. *Chem. Eng. Technol.* **2008**, *31*, 1561–1568.
144. Zöhrer, H.; Mayr, F.; Vogel, F. Stability and performance of ruthenium catalysts based on refractory oxide supports in supercritical water conditions. *Energy Fuels* **2013**, *27*, 4739–4747.
145. Matsumura, Y.; Harada, M.; Nagata, K.; Kikuchi, Y. Effect of heating rate of biomass feedstock on carbon gasification efficiency in supercritical water gasification. *Chem. Eng. Commun.* **2006**, *193*, 649–659.
146. Sınağ, A.; Kruse, A.; Rathert, J. Influence of the heating rate and the type of catalyst on the formation of key intermediates and on the generation of gases during hydropyrolysis of glucose in supercritical water in a batch reactor. *Ind. Eng. Chem. Res.* **2004**, *43*, 502–508.
147. Boukis, N.; Galla, U.; Müller, H.; Dinjus, E. Biomass gasification in supercritical water. Experimental progress achieved with the VERENA pilot plant. In Proceedings of the 15th European Conference & Exhibition, 7–11 May 2007; Volume 7; pp. 1013–1016.
148. Boukis, N.; Galla, U.; D'Jesus, P.; Müller, H.; Dinjus, E. Gasification of wet biomass in supercritical water. Results of pilot plant experiments. In Proceedings of the 14th European Biomass Conference, Paris, France, 17–21 October 2005; pp. 964–967.
149. Chen, J.; Lu, Y.; Guo, L.; Zhang, X.; Xiao, P. Hydrogen production by biomass gasification in supercritical water using concentrated solar energy: System development and proof of concept. *Int. J. Hydrog. Energy* **2010**, *35*, 7134–7141.
150. Liao, B.; Guo, L.; Lu, Y.; Zhang, X. Solar receiver/reactor for hydrogen production with biomass gasification in supercritical water. *Int. J. Hydrog. Energy* **2013**, *38*, 13038–13044.
151. Lu, Y.; Zhao, L.; Guo, L. Technical and economic evaluation of solar hydrogen production by supercritical water gasification of biomass in China. *Int. J. Hydrog. Energy* **2011**, *36*, 14349–14359.
152. Xiao, P.; Guo, L.; Zhang, X.; Zhu, C.; Ma, S. Continuous hydrogen production by biomass gasification in supercritical water heated by molten salt flow: System development and reactor assessment. *Int. J. Hydrog. Energy* **2013**, *38*, 12927–12937.
153. Harinck, J.; Smit, K.G. A Process and a Reaction Apparatus for the Gasification of Wet Biomass. WO Application WO/2013/030026, 7 March 2013.
154. Hong, G.T.; Killilea, W.R.; Thomason, T.B. Method for Solids Separation in a Wet Oxidation Type Process. U.S. Patent 4,822,497, 18 April 1989.
155. Daman, E.L. Process and Apparatus for Supercritical Water Oxidation. U.S. Patent 5,723,045, 3 March 1998.

156. Daman, E.L. Process and Apparatus for Supercritical Water Oxidation. U.S. Patent 5,571,423, 5 November 1996.
157. Marrone, P.A.; Hodes, M.; Smith, K.A.; Tester, J.W. Salt precipitation and scale control in supercritical water oxidation—Part B: Commercial/full-scale applications. *J. Supercrit. Fluids* **2004**, *29*, 289–312.
158. Xu, D.H.; Wang, S.Z.; Gong, Y.M.; Guo, Y.; Tang, X.Y.; Ma, H.H. A novel concept reactor design for preventing salt deposition in supercritical water. *Chem. Eng. Res. Des.* **2010**, *88*, 1515–1522.
159. Schubert, M.; Regler, J.W.; Vogel, F. Continuous salt precipitation and separation from supercritical water. Part 1: Type 1 salts. *J. Supercrit. Fluids* **2010**, *52*, 99–112.
160. Karlsruhe, F. Device for treating Flowable Materials in Super-Critical Water, e.g., for Treating Effluent, Comprises Cylindrical Reactor with Pressure Lines for Introducing Educt and Removing Product. German Patent DE20220307, 30 April 2003.
161. Potic, B.; Kersten, S.R.A.; Ye, M.; van der Hoef, M.A.; Kuipers, J.A.M.; van Swaaij, W.P.M. Fluidization with hot compressed water in micro-reactors. *Chem. Eng. Sci.* **2005**, *60*, 5982–5990.
162. Lu, Y.; Jin, H.; Guo, L.; Zhang, X.; Cao, C.; Guo, X. Hydrogen production by biomass gasification in supercritical water with a fluidized bed reactor. *Int. J. Hydrog. Energy* **2008**, *33*, 6066–6075.
163. Cao, C.; Guo, L.; Jin, H.; Guo, S.; Lu, Y.; Zhang, X. The influence of alkali precipitation on supercritical water gasification of glucose and the alkali recovery in fluidized-bed reactor. *Int. J. Hydrog. Energy* **2013**, *38*, 13293–13299.
164. Harinck, J.; Smit, K.G. A Reaction Apparatus and a Process for the Gasification of Wet Biomass. WO Application WO/2013/030027, 7 March 2013.
165. Harinck, J.; Smit, K.G. A Process for the Gasification of Wet Biomass. WO Application WO/2013/030028, 7 March 2013.